Symmetry, Hopf Bifurcation and the Emergence of Cluster Solutions in Time Delayed Neural Networks

Zhen Wang[1] and Sue Ann Campbell[a)]

Department of Applied Mathematics and Centre for Theoretical Neuroscience, University of Waterloo, Waterloo ON N2L 3G1 Canada

We consider networks of N identical oscillators with time delayed, global circulant coupling, modeled by a system of delay differential equations with Z_N symmetry. We first study the existence of Hopf bifurcations induced by the coupling time delay, and then use symmetric Hopf bifurcation theory to determine how these bifurcations lead to different patterns of symmetric cluster oscillations. We apply our results to a case study: a network of FitzHugh-Nagumo neurons with diffusive coupling. For this model, we derive the asymptotic stability, global asymptotic stability, absolute instability, and stability switches of the equilibrium point in the plane of coupling time delay (τ) and excitability parameter (a). We investigate the patterns of cluster oscillations induced by the time delay, and determine the direction and stability of the bifurcating periodic orbits by employing the multiple time scales method and normal form theory. We find that in the region where stability switching occurs, the dynamics of the system can be switched from the equilibrium point to any symmetric cluster oscillation, and back to equilibrium point as the time delay is increased.

Keywords: delay differential equation; Hopf bifurcation; neural networks; symmetric cluster oscillation; stability analysis

[a)]Corresponding author: sacampbell@uwaterloo.ca; This work was supported by the Natural Sciences and Engineering Research Council of Canada.

This manuscript was accepted by Chaos. Click here to see the version of record.

Clustering is a type of oscillatory network behaviour where elements of the network separate into groups. Elements within a group oscillate synchronously; elements in different groups maintain a fixed phase difference. We show, for a general neural network model with time delayed coupling, how certain cluster solutions arise due to the symmetry of the network. We give explicit formulae for the time delays at which the cluster solutions arise. In a case study of a particular model we show how time delays in the coupling between neurons can give rise to switching between different stable cluster solutions, coexistence of multiple stable cluster solutions and solutions with multiple frequencies. This work gives a possible mechanism for the creation of different rhythms by the same network in the brain – different cluster solutions give rise to different network frequencies.

I. INTRODUCTION

Coupled oscillators arise in a variety of areas including engineering, biology and chemistry. Specific examples include neural networks[1,2], laser arrays[3,4], flashing of fireflies[5], and movement of a slime mode[6]. One of the prevalent behaviours of coupled oscillator systems is phase locking, a state where the elements in the system oscillate with some fixed phase difference. There is a large literature on synchronization, where the phase difference between any two oscillators is zero, (see, e.g., the review paper of Dörfler and Bullo[7] and references therein). However, synchronization is just one of many possible phase-locked solutions that can occur in coupled oscillator systems. Further, synchronization is not always a desirable state[8]. Clustering is a type of phase locking behavior where the oscillators in a network separate into groups where each group consists of fully synchronized oscillators, and different groups are phase-locked with nonzero phase difference.[9,10]. Symmetric clustering refers to the situation where all the groups are the same size.

In realistic coupled systems, there are time delays in the connections between individual oscillators due to the time for information to propagate from one element to the other. In neural networks, this delay is attributed to the transmission of electric activity along an axon or dendrite, or across a synapse. In recent years, there has been considerable research studying clustering in systems with time delays using a variety of techniques. Phase model

analysis can be used in the case where the uncoupled elements are intrinsically oscillating and the coupling is weak[11–15]. Alternatively, the stability of cluster solutions can be analyzed directly using Floquet theory and the properties of the connection matrix[16–21]. When the uncoupled elements are not oscillatory, the emergence of in-phase and anti-phase (1-cluster and 2-cluster) solutions in two cell networks has been studied by bifurcation analysis[22–25].

In many cases, cluster solutions occur in networks of coupled oscillators with symmetry. Symmetric bifurcation theory was first developed by Golubitsky et al.[26] for systems of ordinary differential equations and later extended by Wu[27] to systems with time delays. The key point in such symmetric bifurcation theories is that the patterns of bifurcated equilibria and typical oscillators can be predicted in terms of their symmetry. There has been great interest in applying these results to artificial neural network models with D_N symmetry (especially nearest neighbour coupling)[28–35]. However, little has been done on more general neural oscillator models or on systems with other symmetries. A notable exception is the work of Song and Xu[25] who use symmetric bifurcation theory to study the existence of 1-cluster and 2-cluster solutions in a two cell network of FitzHugh-Nagumo neurons. Further, Buono et al.[36] studied rings of delay-coupled lasers with unidirectional and bidirectional coupling. They use group-theoretic techniques to classify symmetric compound laser modes (CLMs) according to isotropy subgroups, and further study the symmetry-breaking bifurcations from maximally symmetric solutions. We note also the related work of Blyuss et al.[37–39] which uses symmetric bifurcation theory to study the cluster solutions arising in various disease models.

In this paper we investigate how symmetric bifurcation theory can help predict the cluster periodic solutions occurring in time delayed neural oscillator systems. We consider a network of arbitrary size with arbitrary oscillators and time delayed, global circulant coupling. The general model is as follows

$$X_i'(t) = F(X_i(t), X_i(t-\tau_s)) + \sum_{j=1}^{N} w_{ij} G(X_i(t), X_j(t-\tau)),\ i = 1, \cdots, N, \qquad (1)$$

where X_i denotes the variables of a m-dimensional subsystems, τ_s is the self-feedback delay, and τ is the coupling time delay between different nodes. F and G are smooth functions that describe the internal and coupling behavior of the subsystems, respectively. We will focus on models that are relevant to neural networks. Denote $W = (w_{ij}) = circ(w_0, w_1, \cdots, w_{N-1})$. In particular, we take $w_0 = 0$, all w_i to be positive and $w_i \neq w_j$, if $i \neq j$. As we show below,

This manuscript was accepted by Chaos. Click here to see the version of record.

ing structure of W means that the system has $\mathbb{Z}_N$ symmetry.

The rest of this paper is organized as follows. In section II, we determine the critical values of the delay in (1) which lead to Hopf bifurcation. In section III, we investigate the synchronization patterns of the periodic solutions generated by the Hopf bifurcations using the symmetric local Hopf bifurcation theory for delay differential equations. In section IV, we apply the results obtained in previous sections to a particular example: a FitzHugh-Nagumo network with diffusive coupling. We use the method of multiple time scales to determine the stability of bifurcating periodic solutions and compare the theoretical results with numerical simulations for specific parameter values.

II. HOPF BIFURCATIONS INDUCED BY THE COUPLING TIME DELAY

Let $E^* = (X_1^*, \cdots, X_N^*)$ be a symmetric equilibrium point of (1). That is, $X_1^* = \cdots = X_N^* = X^*$ where X^* satisfies $F(X^*, X^*) + \bar{w}G(X^*, X^*) = 0$ with $\bar{w} = \sum_{k=0}^{N-1} w_k$. The linearization of (1) about E^* is given by

$$X_i' = A_1 X_i(t) + A_2 X_i(t-\tau_s) + \sum_{j=1}^{N} w_{ij} B X_j(t-\tau), \ i = 1, \cdots, N. \tag{2}$$

Here A_1, A_2 are the Jacobian matrix of $F(X_i, X_i(t-\tau_s)) + \sum_{j=1}^{N} w_{ij} G(X_i(t), X_j(t-\tau))$ with respect to X_i, $X_i(t-\tau_s)$, evaluated at E^*, respectively. B is the Jacobian matrix of $G(X_i(t), X_j(t-\tau))$ with respect to $X_j(t-\tau)$, evaluated at E^*. Therefore, the characteristic matrix of the linearization (2) is given by

$$\mathcal{M}(\lambda, \tau) = \begin{pmatrix} \lambda I - A_1 - A_2 e^{-\lambda\tau_s} & -e^{-\lambda\tau} w_1 B & \cdots & -e^{-\lambda\tau} w_{N-1} B \\ -e^{-\lambda\tau} w_{N-1} B & \lambda I - A_1 - A_2 e^{-\lambda\tau_s} & \cdots & -e^{-\lambda\tau} w_{N-2} B \\ \vdots & \vdots & \ddots & \vdots \\ -e^{-\lambda\tau} w_1 B & -e^{-\lambda\tau} w_2 B & \cdots & \lambda I - A_1 - A_2 e^{-\lambda\tau_s} \end{pmatrix}$$

where I is the $m \times m$ identity matrix. Note that $\mathcal{M}(\lambda, \tau)$ is a block circulant matrix. We use this structure, inspired by the work of[25,40], to simplify the characteristic equation.

Recall that λ is a root of the characteristic equation if and only if Ker $\mathcal{M}(\lambda, \tau)$ is nonempty, i.e., there is a non-zero vector E such that

$$\mathcal{M}(\lambda, \tau) E = 0. \tag{3}$$

Let ρ be any N-th root of unity, that is

$$\rho \in \{\rho_0, \rho_1, \cdots, \rho_{N-1}\}, \text{ and } \rho_k = e^{i\frac{2\pi}{N}k}, \ k = 0, 1, \cdots, N-1.$$

Let $\xi \in \mathbb{R}^m$. Then the compound vector

$$E = \begin{pmatrix} \xi \\ \rho\xi \\ \vdots \\ \rho^{N-1}\xi \end{pmatrix}$$

satisfies (3) if and only if ξ satisfies $\mathcal{H}\xi = 0$ where

$$\mathcal{H} = \lambda I - A_1 - A_2 e^{-\lambda\tau_s} - e^{\lambda\tau}(w_1\rho + w_2\rho^2 + \cdots + w_{N-1}\rho^{N-1})B.$$

Using the form of the vectors E with $\rho = \rho_k$, $k = 0, \ldots, N-1$, then shows that the characteristic equation of the linearization (2) is

$$\Delta(\lambda, \tau) = \det(\mathcal{M}(\lambda, \tau)) = \prod_{k=0}^{N-1} \Delta_k(\lambda, \tau) = 0, \tag{4}$$

where

$$\Delta_k(\lambda, \tau) = \det(\lambda I - A_1 - A_2 e^{-\lambda\tau_s} - e^{-\lambda\tau}\delta_k B). \tag{5}$$

Here $\delta_k = \sum_{j=1}^{N-1} w_j \rho_k^j$, $k = 0, 1, \cdots, N-1$, are eigenvalues of the connectivity matrix W. Define $\delta_k = \alpha_k + i\beta_k$ and note that $\delta_{N-k} = \overline{\delta_k}$.

For the rest of the paper we will focus on the case of neural oscillators that can be written in the form:

$$\begin{aligned} V_i' &= F_V(V_i, V_i(t-\tau_s), U_i(t)) + \sum_{j=1}^{N} w_{ij} G(V_i(t), V_j(t-\tau)) \\ U_i' &= F_U(V_i, U_i(t)) \end{aligned}$$

where the variable $V_i \in \mathbb{R}$ corresponds to the voltage and the variables $U_i \in \mathbb{R}^{m-1}$ correspond to gating and other variables (such as intracellular ionic concentrations). This includes artificial neural networks with delayed self feedback as considered in[28,41] and networks of conductance based models, such as those we consider in section IV. Since the connectivity is always through the first variable in these models, the matrix B in (2) has all components

except the $B_{1,1}$. In this situation we can describe explicitly how coupling delay gives rise to Hopf bifurcations.

Suppose that the characteristic equation has a pair of pure imaginary eigenvalues. Specifically, for some value of τ, let $i\omega_k$ be a root of $\Delta_k(\lambda,\tau)$ for some $k \in \{0,1,\cdots,N-1\}$. In this situation we have

$$\Delta_k(i\omega_k,\tau) = L(i\omega_k) + H(i\omega_k)\delta_k e^{-i\omega_k\tau}.$$

Separating into real and imaginary parts we have

$$\begin{aligned}(H_R\alpha_k - H_I\beta_k)\cos(\omega_k\tau) + (H_I\alpha_k + H_R\beta_k)\sin(\omega_k\tau) &= -L_R\\ (H_I\alpha_k + H_R\beta_k)\cos(\omega_k\tau) - (H_R\alpha_k - H_I\beta_k)\sin(\omega_k\tau) &= -L_I\end{aligned} \tag{6}$$

where $L_R, L_I,\ H_R, H_I$ denote the real and imaginary parts of $L(i\omega_k)$, and $H(i\omega_k)$, respectively. Note that L_R, H_R are even functions of ω while L_I, H_I are odd. Squaring and adding the above two equations yields

$$L_R^2 + L_I^2 - (H_R^2 + H_I^2)(\alpha_k^2 + \beta_k^2) = 0. \tag{7}$$

There are several possibilities. If δ_k is complex, and then $\Delta_k(\lambda,\tau)$ has a root $i\omega_k$ and $\Delta_{N-k}(\lambda,\tau)$ has a root $-i\omega_k$, corresponding to the roots $\pm\omega_k$ of (7). If δ_k is real, then $\Delta_k(\lambda,\tau)$ has a pair of pure imaginary roots $(\pm i\omega_k)$ corresponding to the roots $\pm\omega_k$ of (7). This is the case for $k = 0$ and $k = \frac{N}{2}$ (for N even). If δ_k is real and $k \neq 0, \frac{N}{2}$ then $\Delta_k(\lambda,\tau) = \Delta_{N-k}(\lambda,\tau)$ and both have a pair of purely imaginary roots $(\pm i\omega_k)$, thus $\Delta(\lambda,\tau)$ has a repeated pair of pure imaginary roots. This will occur, for example, if the connection matrix W is symmetric as well as circulant. In all cases, it is enough to consider $\Delta_k(\lambda,\tau),\ k = 0,1,\ldots,\lfloor\frac{N}{2}\rfloor$ to determine all the roots of $\Delta(\lambda,\tau)$ with pure imaginary real parts.

Provided that ω_k exists, (6) may be solved for the corresponding value of τ

$$\begin{aligned}\tau_{k,j} &= \frac{1}{\omega_k}\left(2\pi j - \psi_k + \arccos\left(\frac{-L_R}{\sqrt{(H_R^2+H_I^2)(\alpha_k^2+\beta_k^2)}}\right)\right), \text{ if } L_I > 0\\ &= \frac{1}{\omega_k}\left(2\pi(j+1) - \psi_k - \arccos\left(\frac{-L_R}{\sqrt{(H_R^2+H_I^2)(\alpha_k^2+\beta_k^2)}}\right)\right), \text{ if } L_I < 0\end{aligned} \tag{8}$$

with

$$\psi_k = \arg(H(i\omega)\delta_k).$$

We now have the following result.

Theorem II.1. *Assume that the characteristic equation* (4) *has a simple pair of pure imaginary roots* $\pm i\omega_k$ *when* $\tau = \tau_{k,j}$ *as defined in* (8)*, and all other roots* λ *satisfy* $\lambda \neq l\omega_k$ *for any integer* l*. Assume*

$$|L(i\omega)|^2[H_R(\omega)H_R'(\omega) + H_I(\omega)H_I'(\omega)] - |H(\omega)|^2[L_R(\omega)L_R'(\omega) + L_I(\omega)L_I'(\omega)] \neq 0.$$

Then, (1) *undergoes a Hopf bifurcation near the equilibrium point* E^* *at each critical value* $\tau_{k,j}$*.*

Proof. Straightforward calculations show that

$$\mathrm{Re}\left[\frac{d\lambda(\tau)}{d\tau}\Big|_{\tau=\tau_{k,j}}\right] \neq 0$$

if and only if

$$|L(i\omega)|^2[H_R(\omega)H_R'(\omega) + H_I(\omega)H_I'(\omega)] - |H(\omega)|^2[L_R(\omega)L_R'(\omega) + L_I(\omega)L_I'(\omega)] \neq 0.$$

The result then follows from the standard Hopf bifurcation theorem for delay differential equations[42]. □

III. PATTERNS OF BIFURCATING PERIODIC SOLUTIONS

In this section, we investigate the patterns of periodic solutions arising in the Hopf bifurcation described above. To do this, we must reformulate (1) and study its symmetry. Set $u(t) = (X_1(t), \cdots, X_N(t))^T$ and define $u_t(\vartheta) = u(t+\vartheta)$, for $\vartheta \in [-\tau, 0]$. Let $u_t \in \mathcal{C} = C([-\tau, 0], \mathbb{R}^{mN})$, the Banach space of continuous mapping from $[-\tau, 0]$ to $\mathbb{R}^{mN}$ equipped with supremum norm. Then (1) can be rewritten

$$u'(t) = h(u_t) \tag{9}$$

where

$$h_i(\phi) = F_k(\phi_l(0), \phi_l(-\tau_s)) + \sum_{j=1}^{N} w_{lj} G_k(\phi_l(0), \phi_j(-\tau)) \tag{10}$$

with $i = lm + k,\ l = 0, \ldots, N-1,\ k = 0, \ldots, m-1$. Similarly, the linearization (2) may be rewritten

$$u'(t) = \mathcal{L}(\tau)u_t \tag{11}$$

where

$$\mathcal{L}(\tau)\phi = (A_1 \otimes I_m)\phi(0) + (A_2 \otimes I_m)\phi(-\tau_s) + \epsilon(W \otimes B)\phi(-\tau) \tag{12}$$

where I_m is the $m \times m$ identity matrix, and "$\otimes$ " represents the Kronecker product of matrices. From standard theory[42], this linear system generates a strongly continuous semigroup of linear operators on $\mathcal{C}$ with infinitesimal generator, $\mathcal{A}$, defined by

$$\mathcal{A}(\tau)\phi = \dot{\phi}, \ \phi \in \mathrm{Dom}(A)$$
$$\mathrm{Dom}(\mathcal{A}(\tau)) = \{\phi \in \mathcal{C} : \dot{\phi} \in \mathcal{C}, \dot{\phi}(0) = \mathcal{L}(\tau)\phi\}.$$

Let Γ be a group acting on $\mathbb{R}^{mN}$. It follows that (9) is Γ-equivariant if $h(\gamma u_t) = \gamma h(u_t)$ for all $\gamma \in \Gamma$[26,27]. From (10), the symmetry of (9) is determined by the symmetry of the connection matrix W. We will focus on the case where W is circulant but does not possess any other symmetry. Thus we consider $\Gamma = \mathbb{Z}_N$, the cyclic group of order N, with generator γ, where the action of $\mathbb{Z}_N$ on $\mathbb{R}^{mN}$ is given by

$$(\gamma u)_i = u_{i-m}, \ \text{for } i, i-m \bmod Nm,$$

where u_i is the ith component of u. Then it is easy to verify that both (9) and (11) are $\mathbb{Z}_N$ equivariant.

Suppose that when $\tau = \tau_{k,j}$ the characteristic equation (4) has a pair of pure imaginary roots, $\pm i\omega_k$, with corresponding vectors, $\xi_k, \bar{\xi}_k \in \mathrm{Ker}\ \mathcal{M}(i\omega, \tau_{k,j})$, as described in the previous section. Then $\mathcal{A}(\tau_{k,j})$ has eigenvalues $\pm i\omega_k$ and the corresponding generalized eigenspace, $U_{i\omega_k}$, is spanned by the eigenfunctions $\mathrm{Re}(e^{i\omega_k\theta}\xi_k)$, $\mathrm{Im}(e^{i\omega_k\theta}\xi_k)$[27,42].

Lemma III.1. *Assume that for one and only one* $k \in 0, 2, \ldots, \lfloor \frac{N}{2} \rfloor$ *and some* $j \in \mathbb{Z}_0^+$, $\tau = \tau_{k,j} > 0$ *as defined in (8), i.e., the characteristic equation* (4) *has a simple pair of pure imaginary roots* $\pm i\omega_k$. *Then*

$$\dim \mathrm{Ker}\ \mathcal{M}(\pm i\omega_k, \tau_{k,j}) = 2,$$

and the restricted action of $\mathbb{Z}_N$ *on* $\mathrm{Ker}\ \mathcal{M}(i\omega_k, \tau_{k,j})$ *is isomorphic to the action of* $\mathbb{Z}_N$ *on* $\mathbb{R}^2$.

Proof. It follows from the discussion of the previous section that

$$\mathrm{Ker}\ \mathcal{M}(i\omega_k, \tau_{k,j}) = \{(y_1 + iy_2)\xi_k; \ y_1, y_2 \in \mathbb{R}\}.$$

Further, $\mathbb{R}$ is an absolutely irreducible representation of $\mathbb{Z}_N$[26]. Define $J : \mathrm{Ker}\ \mathcal{M}(i\omega_k, \tau_{k,j}) \cong \mathbb{R}^2$ as

$$J((y_1 + iy_2)\xi_k) = (y_1, y_2)^T.$$

Clearly, J is a linear isomorphism. Note that

$$\gamma((y_1 + iy_2)\xi_k) = (y_1 + iy_2)\gamma(\xi_k) = \rho_k^{N-1}(y_1 + iy_2)\xi_k.$$

Consequently

$$J[\gamma((y_1 + iy_2)\xi_k)] = \gamma[J((y_1 + iy_2)\xi_k)].$$

This completes the proof. □

Let $\mathcal{T} = \frac{2\pi}{\omega_k}$, and denote by $P_{\mathcal{T}}$ the Banach space of continuous $\mathcal{T}$-periodic mappings, $u : \mathbb{R} \to \mathbb{R}^{mN}$, and by $SP_{\mathcal{T}}$ the subspace of $P_{\mathcal{T}}$ consisting of all $\mathcal{T}$-periodic solutions of (11) when $\tau = \tau_{k,j}$. Specifically,

$$SP_{\mathcal{T}} = \big\{x_1\epsilon_1(t) + x_2\epsilon_2(t),\ x_1, x_2 \in \mathbb{R}\big\}, \tag{13}$$

where

$$\epsilon_1(t) = \cos(\omega_k t)\mathrm{Re}(\xi_k) - \sin(\omega_k t)\mathrm{Im}(\xi_k),$$
$$\epsilon_2(t) = \sin(\omega_k t)\mathrm{Re}(\xi_k) + \cos(\omega_k t)\mathrm{Im}(\xi_k).$$

Let S^1 be the circle group. Then $\mathbb{Z}_N \times S^1$ acts on $P_{\mathcal{T}}$ (and hence, $SP_{\mathcal{T}}$) as follows

$$(\gamma, \theta)u(t) = \gamma u(t + \theta),\ \gamma \in \mathbb{Z}_N, \theta \in [0, \mathcal{T}). \tag{14}$$

For any $\theta \in (0, \mathcal{T})$, let Σ^θ be the subgroup of $\mathbb{Z}_N \times S^1$ generated by (γ, θ). Its fixed point set is given by

$$\mathrm{Fix}(\Sigma^\theta, SP_{\mathcal{T}}) = \big\{u \in SP_{\mathcal{T}}, (\gamma, \theta)u(t) = u(t)\big\}. \tag{15}$$

Lemma III.2. *Assume that the characteristic equation* (4) *has a simple pair of pure imaginary roots* $\pm i\omega_k$. *If* $\theta = \frac{k}{N}\mathcal{T}$, *then* $Fix(\Sigma^\theta, SP_{\mathcal{T}}) = SP_{\mathcal{T}}$, *otherwise* $Fix(\Sigma^\theta, SP_{\mathcal{T}}) = 0$. *Moreover,*

$$dim(Fix(\Sigma^\theta, SP_{\mathcal{T}})) = \begin{cases} 2, & \text{if } \theta = \frac{k}{N}\mathcal{T}, \\ 0, & \text{otherwise.} \end{cases}$$

Proof. To begin, note that

$$\gamma(\mathrm{Re}(\xi_k)) = \cos\frac{2\pi k}{N}\mathrm{Re}(\xi_k) + \sin\frac{2\pi k}{N}\mathrm{Im}(\xi_k),$$
$$\gamma(\mathrm{Im}(\xi_k)) = -\sin\frac{2\pi k}{N}\mathrm{Re}(\xi_k) + \cos\frac{2\pi k}{N}\mathrm{Im}(\xi_k).$$

Therefore,

$$\begin{aligned}\gamma(x_1\epsilon_1(t) + x_2\epsilon_2(t)) &= x_1\cos(\omega_k t)\gamma(\mathrm{Re}(\xi_k)) - \sin(\omega_k t)\gamma(\mathrm{Im}(\xi_k)) \\ &\quad + x_2\sin(\omega_k t)\gamma(\mathrm{Re}(\xi_k)) + \cos(\omega_k t)\gamma(\mathrm{Im}(\xi_k)) \\ &= (x_1\cos\frac{2\pi k}{N} - x_2\sin\frac{2\pi k}{N})\epsilon_1(t) + (x_1\sin\frac{2\pi k}{N} + x_2\cos\frac{2\pi k}{N})\epsilon_2(t).\end{aligned}$$

Further, straightforward calculations show that

$$(x_1\epsilon_1 + x_2\epsilon_2)(t+\theta) = (x_1\cos(\omega_k\theta) + x_2\sin(\omega_k\theta))\epsilon_1(t) + (-x_1\sin(\omega_k\theta) + x_2\cos(\omega_k\theta))\epsilon_2(t).$$

Now consider

$$\gamma(x_1\epsilon_1(t) + x_2\epsilon_2(t)) = (x_1\epsilon_1 + x_2\epsilon_2)(t+\theta). \tag{16}$$

In order for this to hold we must have

$$x_1\cos\frac{2\pi k}{N} - x_2\sin\frac{2\pi k}{N} = x_1\cos(\omega_k\theta) + x_2\sin(\omega_k\theta),$$
$$x_1\sin\frac{2\pi k}{N} + x_2\cos\frac{2\pi k}{N} = -x_1\sin(\omega_k\theta) + x_2\cos(\omega_k\theta).$$

Solving the above two equations, we obtain

$$\theta = \frac{(N-k)\mathcal{T}}{N} \text{ and } x_1, x_2 \in \mathbb{R}, \text{or}$$
$$\theta \neq \frac{(N-k)\mathcal{T}}{N} \text{ and } x_1 = x_2 = 0.$$

Note that $\gamma u(t) = u(t + \frac{(N-k)\mathcal{T}}{N})$ if and only if $\gamma u(t + \frac{k\mathcal{T}}{N}) = u(t)$. The conclusion follows. □

From Lemma III.1, and III.2, we can apply the symmetric local Hopf bifurcation theorem for delay differential equation[27] (Theorem 2.1) to obtain the following results.

Theorem III.1. *Assume the conditions of Theorem II.1 are satisfied. The spatio-temporal symmetry of the periodic solution of (1) arising in the Hopf bifurcation at $\tau = \tau_{k,j}$ is determined by $Fix(\Sigma^\theta, SP_\mathcal{T})$ as described in Lemma III.2. Specifically, we have the following*

(1) For $\tau = \tau_{0,j} > 0$, there exists a bifurcation of periodic solutions of (1) with period near $\frac{2\pi}{\omega_k}$, and satisfying

$$u_{i-pm}(t) = u_i(t), \ \ i = 1, 2, \ldots, m, \ \ p = 1, \ldots, N-1,$$

which is the in-phase (1-cluster) periodic solution.

(2) For $\tau = \tau_{k,j} > 0$ such that k and N are relatively prime, there exists a bifurcation of N-cluster periodic solutions of (1). These solutions satisfy

$$u_{i-pm}(t) = u_i(t - p\tfrac{k\mathcal{T}}{N}),\ i = 1, 2, \ldots, m,\ p = 1, \ldots, N-1.$$

where $\mathcal{T}$ is near $\frac{2\pi}{\omega_k}$.

(3) For $\tau_{k,j}$ such that k and N have greatest common factor $b > 1$, there exists a bifurcation of n-cluster periodic solutions of (1). These solutions satisfy

$$u_{i-pm}(t) = u_i(t - p\tfrac{l\mathcal{T}}{n}),\ i = 1, 2, \ldots, m,\ p = 1, \ldots, N-1.$$

where $n = N/b$, $l = k/b$ and $\mathcal{T}$ is near $\frac{2\pi}{\omega_k}$.

Remark III.1. *We have focussed on the case of minimal symmetry in W. The case that W has more symmetry can be dealt with analogously. For example, when W is symmetric and circulant the system (1) has D_n symmetry. In this case, the additional symmetry leads to multiple pairs of pure imaginary eigenvalues and the standard Hopf bifurcation theorem does not apply. However, analysis similar to that carried out in this section can be done and the symmetric local Hopf bifurcation theorem[27] may be applied. This has been done for artificial neural network models with delay[27,30,41].*

IV. APPLICATION TO A FITZHUGH-NAGUMO NETWORK.

In this section, we apply the theory of the previous sections to the following network of FitzHugh-Nagumo neurons:

$$\begin{aligned} \mu x_i' &= x_i - \frac{x_i^3}{3} - y_i + \epsilon \sum_{j=1}^{N} w_{ij}(x_j(t-\tau) - x_i(t)) \\ y_i' &= x_i + a, \quad i = 1, 2, \cdots, N. \end{aligned} \tag{17}$$

Here a is an excitability parameter whose value defines whether the system is excitable ($|a| > 1$), or exhibits self-sustained periodic firing ($|a| < 1$), and $\mu > 0$ is the time-scale parameter, which is usually chosen to be much smaller than unity, corresponding to fast activator variables, x_i, and slow inhibitor variables, y_i[43,44]. The coupling is diffusive/electrical, i.e.,

each pair of neurons is linearly coupled with coupling strength ϵ. The connectivity matrix $W = (w_{ij})$ describes how information is distributed between neurons.

In the model (17) there is a unique symmetric equilibrium point given by $E^* = (x^*, y^*, \cdots, x^*, y^*)^T$ with $x^* = -a$, $y^* = -a + \frac{a^3}{3}$. The linearization of (17) at this equilibrium point is given by (2) with

$$A_1 = \begin{pmatrix} \frac{1}{\mu}(1 - a^2 - \epsilon\bar{w}) & -\frac{1}{\mu} \\ 1 & 0 \end{pmatrix}, \; A_2 = 0, \; B = \begin{pmatrix} \frac{\epsilon}{\mu} & 0 \\ 0 & 0 \end{pmatrix}.$$

Hence the characteristic equation is given by (4) with

$$\Delta_k = \lambda^2 + pr\lambda + r - \epsilon r \delta_k \lambda e^{-\lambda\tau} \tag{18}$$

where $p = a^2 - 1 + \epsilon\bar{w}$, $r = \frac{1}{\mu} > 0$, $\bar{w} = \sum_{j=1}^{N-1} w_{ij} = \sum_{k=1}^{N-1} w_k$, and δ_k is as defined in section II.

A. Distribution of roots of the characteristic equation in the complex plane

It is well-known that the number of roots (counting their multiplicity) of equation (4) in the open right half plane $\{\lambda \in \mathbb{C}, Re\lambda \geq 0\}$ can change only if a root appears on, or crosses the imaginary axis. Thus, the condition guaranteeing that (4) has a root with zero real part will play a key role in the analysis of the distribution of roots.

Straightforward calculations lead to the following

Lemma IV.1. *Assume that $\tau = 0$ and let $\mathcal{I}_N = \{0, 1, \ldots, \lfloor \frac{N}{2} \rfloor\}$. Then we have*

1. *All $2N$ roots of (4) have negative real parts if $\epsilon(\alpha_k - \bar{w}) < a^2 - 1$, for all $k \in \mathcal{I}_N$.*

2. *At least one root of (4) has positive real part if $\epsilon(\alpha_k - \bar{w}) > a^2 - 1$ for some $k \in \mathcal{I}_N$.*

3. *If $\epsilon(\alpha_k - \bar{w}) = a^2 - 1$, for $k = 0$ or $k = N/2$ (N even), (4) has a pair of purely imaginary roots $\pm i\sqrt{r}$.*

4. *If $\epsilon(\alpha_k - \bar{w}) = a^2 - 1$, for some $k = 1, \cdots, \lfloor \frac{N-1}{2} \rfloor$, then (4) has two pairs of purely imaginary roots $\pm i\frac{\epsilon\beta_k \pm \sqrt{\epsilon^2\beta_k^2 + 4\mu}}{2\mu}$*

This manuscript was accepted by Chaos. Click here to see the version of record.

In the following, we seek the condition such that (4) has purely imaginary roots when $\tau > 0$. That is, for some $k \in \mathcal{I}_N$, Δ_k has purely imaginary roots. Noting that

$$L(i\omega) = \frac{1}{\mu} - \omega^2 + i\frac{\omega p}{\mu}, \quad H(i\omega) = -i\frac{\omega\epsilon}{\mu}$$

we define $\omega_k^{\pm}$ and $\tau_{k,j}^{\pm}$, as follows:

$$\omega_k^{\pm} = \frac{\sqrt{2}}{2\mu}\sqrt{(2\mu - p^2 + \epsilon^2|\delta_k|^2) \pm \sqrt{(2\mu - p^2 + \epsilon^2|\delta_k|^2)^2 - 4\mu^2}} \tag{19}$$

and

$$\begin{aligned} \tau_{k,j}^{+} &= \frac{1}{\omega_k^{+}}\left[2\pi(j+1) - \psi_k - \arccos\left(\frac{a^2 - 1 + \epsilon\bar{w}}{\epsilon|\delta_k|}\right)\right], \\ \tau_{k,j}^{-} &= \frac{1}{\omega_k^{-}}\left[2\pi j - \psi_k + \arccos\left(\frac{a^2 - 1 + \epsilon\bar{w}}{\epsilon|\delta_k|}\right)\right], \end{aligned} \tag{20}$$

and $\hat{\tau}_{k,j}^{\pm} = \tau_{k,j}^{\pm} - \frac{2\psi_k}{\omega_k^{\pm}}$, where

$$\psi_k = \arg(\delta_k).$$

Then, Lemma IV.1 and the results of section II give the following.

Lemma IV.2. *for $k \in \mathcal{I}_N$ and $j \in \mathbb{Z}_0^+ = \{0, 1, \ldots\}$,*

1. *If $|\epsilon||\delta_k| < \mu|p|$, the equation $\Delta_k = 0$ has no purely imaginary roots for all $\tau \geq 0$.*

2. *If $|\epsilon||\delta_k| > \mu|p|$, the equation $\Delta_k = 0$ has purely imaginary roots $i\omega_k^{\pm}$ ($-i\omega_k^{\pm}$) at $\tau = \tau_{k,j}^{\pm}$ ($\hat{\tau}_{k,j}^{\pm}$) and the equation $\Delta_{N-k} = 0$ has purely imaginary roots $-i\omega_k^{\pm}$ ($i\omega_k^{\pm}$) at $\tau = \tau_{k,j}^{\pm}$ ($\hat{\tau}_{k,j}^{\pm}$).*

3. *If $\epsilon|\delta_k| = -\mu p$ then $\omega_k^{+} = \omega_k^{-} = \sqrt{r}$ and $\tau_{k,j}^{+} = \tau_{k,j}^{-}$. If $\epsilon|\delta_k| = \mu p$ then $\omega_k^{+} = \omega_k^{-} = \sqrt{r}$ and $\tau_{k,j}^{+} = \tau_{k,j+1}^{-}$.*

4. *Let $\lambda(\tau) = \eta(\tau) + i\omega(\tau)$ be a solution of the equation $\Delta_k = 0$ satisfying $\eta(\tau_{k,j}^{\pm}) = 0$ and $\omega(\tau_{k,j}^{\pm}) = \omega_k^{\pm}$, then we have*

$$Re\left(\left.\frac{d\lambda}{d\tau}\right|_{\tau=\tau_{k,j}^{+},\hat{\tau}_{k,j}^{+}}\right) \geq 0, \quad Re\left(\left.\frac{d\lambda}{d\tau}\right|_{\tau=\tau_{k,j}^{-},\hat{\tau}_{k,j}^{-}}\right) \leq 0,$$

with equality occurring only when $|\epsilon||\delta_k| = \mu|p|$.

Remark IV.1. *When $\epsilon < 0$, the above statements remain true with*

$$\tau^+_{k,j} = \frac{1}{\omega^+_k}\left[2\pi j + \psi_k + \arccos\left(\frac{a^2 - 1 + \epsilon\bar{w}}{\epsilon|\delta_k|}\right)\right],$$
$$\tau^-_{k,j} = \frac{1}{\omega^-_k}\left[(2j+2)\pi + \psi_k - \arccos\left(\frac{a^2 - 1 + \epsilon\bar{w}}{\epsilon|\delta_k|}\right)\right],$$

If $\epsilon|\delta_k| = \mu p$ then $\omega^+_k = \omega^-_k = \sqrt{r}$ and $\tau^+_{k,j+1} = \tau^-_{k,j}$.

We can now completely describe the stability of E^* and the Hopf bifurcations.

Theorem IV.1. *Assume that $\omega^\pm_k$ and $\tau^\pm_{k,j}$ are defined as in (19) and (20), respectively.*

1. *If $|a| > 1$ and $\epsilon > \frac{1-a^2}{2\bar{w}}$, then the equilibrium point E^* is asymptotically stable for all $\tau \in [0, \infty)$.*

2. *If either $|a| > 1$ and $\epsilon < \frac{1-a^2}{\bar{w}-|\delta_k|}$ for some $k \in \mathcal{I}_N \setminus \{0\}$, or $|a| < 1$ and $\epsilon < \frac{1-a^2}{\bar{w}+|\delta_k|}$ for some $k \in \mathcal{I}_N$, then the equilibrium point E^* is unstable for all $\tau \in [0, \infty)$.*

3. *If either $|a| > 1$ and $\epsilon < \frac{1-a^2}{2\bar{w}}$ or $|a| < 1$ and $\epsilon > \frac{1-a^2}{2\bar{w}}$ then the system undergoes Hopf bifurcation at the equilibrium point E^* for $\tau = \tau^+_{0,j}$ and $\tau = \tau^-_{0,m}$, for all $j, m \in \mathbb{Z}^+_0$ such that $\tau^+_{0,j} \neq \tau^\pm_{p,s}$ for any $p \in \mathcal{I}_N, s \in \mathbb{Z}^+_0$ and $\tau^-_{0,m} \neq \tau^\pm_{q,t}$ for any $q \in \mathcal{I}_N, t \in \mathbb{Z}^+_0$.*

4. *If either $|a| > 1$ and $\frac{1-a^2}{\bar{w}-|\delta_k|} < \epsilon < \frac{1-a^2}{\bar{w}+|\delta_k|}$ for some $k \in \mathcal{I}_N \setminus \{0\}$, or $|a| < 1$ and $\epsilon > \frac{1-a^2}{\bar{w}+|\delta_k|}$ for some $k \in \mathcal{I}_N \setminus \{0\}$, then system (17) undergoes Hopf bifurcation near the equilibrium point E^* at $\tau = \tau^+_{k,j}$ and $\tau = \tau^-_{k,m}$, for all $j, m \in \mathbb{Z}^+_0$ such that $\tau^+_{k,j} \neq \tau^\pm_{p,s}$ for any $p \in \mathcal{I}_N, s \in \mathbb{Z}^+_0$ and $\tau^-_{k,m} \neq \tau^\pm_{q,t}$ for any $q \in \mathcal{I}_N, t \in \mathbb{Z}^+_0$.*

Proof. The proof follows from Lemma IV.2 and consideration of the roots of the characteristic equation. □

We now use a Lyapunov functional to establish a global stability result for the equilibrium point E^*. First, letting $x_i + a \mapsto \tilde{x}_i$, $y_i + a - \frac{a^3}{3} \mapsto \tilde{y}_i$, and dropping the $\tilde{}$ for simplicity, we transform E^* to a zero equilibrium point for the following system

$$\begin{aligned} x_i' &= \frac{1}{\mu}\Big[(1 - a^2 - \epsilon\bar{w})x_i - y_i + \epsilon\sum_{j=1}^{N} w_{ij}x_j(t-\tau) + ax_i^2 - \frac{x_i^3}{3}\Big] \\ y_i' &= x_i. \end{aligned} \tag{21}$$

Theorem IV.2. *If $|a| > 2$ and $\epsilon > \frac{4-a^2}{8\bar{w}}$, the equilibrium point E^* of (17) is globally asymptotically stable.*

This manuscript was accepted by Chaos. Click here to see the version of record.

Proof. Define

$$V(x,y)(t) = \mu \sum_{i=1}^{N} x_i^2(t) + \sum_{i=1}^{N} y_i^2(t) + |\epsilon| \sum_{i=1}^{N} \left(\sum_{j=1}^{N} w_{ij} \int_{t-\tau}^{t} x_j^2(v) dv \right).$$

Thus

$$\begin{aligned}
\frac{dV}{dt} &= 2\mu \sum_{i=1}^{N} x_i(t)x'(t) + 2\sum_{i=1}^{N} y_i(t)y'(t) + |\epsilon| \sum_{i=1}^{N} \left(\sum_{j=1}^{N} w_{ij}(x_j^2(t) - x_j^2(t-\tau)) \right) \\
&= 2\sum_{i=1}^{N} (1 - a^2 - \epsilon\bar{w}) x_i^2 - 2\sum_{i=1}^{N} x_i y_i + \epsilon \sum_{i=1}^{N} \sum_{j=1}^{N} 2w_{ij} x_i x_j(t-\tau) + 2a \sum_{i=1}^{N} x_i^3 \\
&\quad - 2/3 \sum_{i=1}^{N} x_i^4 + 2\sum_{i=1}^{N} y_i x_i + |\epsilon| \sum_{i=1}^{N} \left(\sum_{j=1}^{N} w_{ij}(x_j^2(t) - x_j^2(t-\tau)) \right) \\
&\leq \sum_{i=1}^{N} 2(1 - a^2 - \epsilon\bar{w}) x_i^2 + |\epsilon| \sum_{i=1}^{N} \left(\sum_{j=1}^{N} w_{ij}(x_i^2(t) + x_j^2(t-\tau)) \right) - 2/3 \sum_{i=1}^{N} x_i^4 \\
&\quad + \sum_{i=1}^{N} (3a^2/2x_i^2 + 2/3x_i^4) + |\epsilon| \sum_{i=1}^{N} \left(\sum_{j=1}^{N} w_{ij}(x_j^2(t) - x_j^2(t-\tau)) \right) \\
&= \sum_{i=1}^{N} (2 - 1/2a^2 - 2\epsilon\bar{w} + 2|\epsilon|\bar{w}) x_i^2(t).
\end{aligned}$$

If $\epsilon \geq 0$, the zero equilibrium point of (21) is globally asymptotically stable if $2 - 1/2a^2 < 0$; and if $\epsilon < 0$, the zero equilibrium point is globally asymptotically stable if $2 - 1/2a^2 - 4\epsilon\bar{w} < 0$. Since the zero equilibrium point has the same stability as E^* of (17), we have the conclusion of the theorem.

□

The Hopf bifurcations described by Theorem IV.1 create cluster periodic solutions, as described by Theorem III.1. To understand how this effects the dynamics of the system, we need to determine the stability of these solutions, which we do in the next section.

B. Direction and stability of Hopf bifurcations

In this section, we first derive the normal form for a Hopf bifurcation, using the multiple time scales method and taking the time delay as bifurcation parameter. We then give a bifurcation analysis based on the normal form.

As discussed above, system (17) undergoes Hopf bifurcations when $\tau = \tau_{k,j}^{\pm}$. Here we denote $\tau_{k,j}^{\pm} = \tau_k$ for simplicity. In this section, we assume that the characteristic equation

This manuscript was accepted by Chaos. Click here to see the version of record.

(4) has a pair of pure imaginary roots $\pm\omega_k^{\pm}$ at τ_k, and all the other eigenvalues have negative real parts.

Defining $u(t) = (u_1(t), \cdots, u_{2N}(t))^T = (x_1(t), y_1(t), \cdots, x_N(t), y_N(t))^T$, system (21) can be rewritten as

$$u' = N_0 u(t) + N_1 u(t-\tau) + f(u(t)), \tag{22}$$

where

$$N_0 = \begin{Bmatrix} M & 0 & \cdots & 0 \\ 0 & M & \cdots & 0 \\ \vdots & \vdots & \ddots & \vdots \\ 0 & 0 & \cdots & M \end{Bmatrix}, N_1 = \frac{\epsilon}{\mu}\begin{Bmatrix} 0 & \bar{w_1} & \bar{w_2} & \cdots & \bar{w_{N-1}} \\ \bar{w_{N-1}} & 0 & \bar{w_1} & \cdots & \bar{w_{N-2}} \\ \vdots & \vdots & \vdots & \ddots & \vdots \\ \bar{w_1} & \bar{w_2} & \bar{w_3} & \cdots & 0 \end{Bmatrix}, \text{ and } f(u(t)) = \frac{1}{\mu}\begin{bmatrix} au_1^2 - \frac{u_1^3}{3} \\ 0 \\ \vdots \\ au_{2N-1}^2 - \frac{u_{2N-1}^3}{3} \\ 0 \end{bmatrix}$$

with

$$M = \begin{bmatrix} \frac{1-a^2-\epsilon\bar{w}}{\mu} & -\frac{1}{\mu} \\ 1 & 0 \end{bmatrix}, \text{and } \bar{w_i} = \begin{bmatrix} w_i & 0 \\ 0 & 0 \end{bmatrix}, \ i = 1, \cdots, N-1.$$

Defining

$$\tau = \tau_k + \zeta^2 \tau_2, \tag{23}$$

we seek a second-order uniform expansion of the solution of equation (22) in the neighborhood of $\tau = \tau_k$ in the form

$$u(t;\zeta) = \zeta u_1(T_0, T_2) + \zeta^2 u_2(T_0, T_2) + \zeta^3 u_3(T_0, T_2). \tag{24}$$

Here $T_0 = t$, $T_1 = \zeta t$, $T_2 = \zeta^2 t$, and ζ is a dimensional bookkeeping parameter. Note that the solution does not depend on the slow scale T_1 because secular terms first appear at $\mathcal{O}(\zeta^3)$. In this case, the derivative with respect to t is transformed into

$$\frac{d}{dt} = \frac{\partial}{\partial T_0} + \zeta^2 \frac{\partial}{\partial T_2} = D_0 + \zeta^2 D_2,$$

with $D_i = \frac{\partial}{T_i}$, $i = 0, 2$. Substituting (24) into $f(u(t,\zeta))$ yields

$$f(u(t,\zeta)) = \sum_{k\geq 2} \zeta^k f_k(u_1(T_0,T_2), u_2(T_0,T_2), u_3(T_0,T_2)). \tag{25}$$

Moreover, we express $u(t-\tau)$ in terms of the scales T_0 and T_2 as

$$u(t-\tau,\zeta) = \zeta u_1(T_0 - \tau, T_2 - \zeta^2\tau) + \zeta^2 u_2(T_0 - \tau, T_2 - \zeta^2\tau) + \zeta^3 u_3(T_0 - \tau, T_2 - \zeta^2\tau)$$

This manuscript was accepted by Chaos. Click here to see the version of record.

which upon expansion for small ζ becomes

$$u(t-\tau,\zeta) = \zeta u_{1\tau} + \zeta^2 u_{2\tau} + \zeta^3(u_{3\tau} - \tau_2 D_0 u_{1\tau} - \tau_k D_2 u_{1\tau}) \tag{26}$$

with $u_{i\tau} = u_i(T_0 - \tau_k, T_2)$, $i = 1, 2, 3$. Substituting equations (24) - (26) into equation (22), and equating coefficients of like powers of ζ yields

$$D_0 u_1 - N_0 u_1 - N_1 u_{1\tau} = 0, \tag{27}$$

$$D_0 u_2 - N_0 u_2 - N_1 u_{2\tau} = f_2, \tag{28}$$

$$D_0 u_3 - N_0 u_3 - N_1 u_{3\tau} = -D_2 u_1 - \tau_2 N_1 D_0 u_{1\tau} - \tau_k N_1 D_2 u_{1\tau} + f_3, \tag{29}$$

The general solution of equation (27) is

$$u_1 = A_k(T_2)\mathbf{p_k} e^{i\omega_k T_0} + \bar{A}_k(T_2)\bar{\mathbf{p}}_\mathbf{k} e^{-i\omega_k T_0}, \tag{30}$$

where $\mathbf{p_k}$ is given by

$$\mathbf{p_k} = (i\omega_k, 1, i\omega_k\rho_k, \rho_k, \cdots, i\omega_k\rho_k^{N-1}, \rho_k^{N-1})^T, \tag{31}$$

with $\rho_k = e^{\frac{i2\pi}{N}k}$. Substituting equation (30) into equation (28) yields

$$D_0 u_2 - N_0 u_2 - N_1 u_{2\tau} = \frac{a\omega_k^2}{\mu}\big[- A^2 e^{2i\omega_k T_0}\boldsymbol{\alpha} + A\bar{A}\boldsymbol{\beta}\big] + c.c, \tag{32}$$

where $c.c$ stands for the complex conjugate of the preceding terms and

$$\boldsymbol{\alpha} = (1, 0, \rho_k^2, 0, \cdots, \rho_k^{2(N-1)}, 0)^T,$$

$$\boldsymbol{\beta} = (1, 0, 1, 0, \cdots, 1, 0)^T.$$

A particular solution of (32) has the form

$$u_2 = \alpha_1 e^{2i\omega_k T_0} + \beta_1 + c.c. \tag{33}$$

Substituting (33) into (32), and balancing similar terms, we have

$$u_2 = \gamma e^{2i\omega_k T_0}\begin{bmatrix} 1 \\ \frac{1}{2i\omega_k} \\ \rho_k^2 \\ \frac{1}{2i\omega_k}\rho_k^2 \\ \vdots \\ \rho_k^{2(N-1)} \\ \frac{1}{2i\omega_k}\rho_k^{2(N-1)} \end{bmatrix} + a\omega_k^2 A\bar{A}\begin{bmatrix} 0 \\ 1 \\ 0 \\ 1 \\ \vdots \\ 0 \\ 1 \end{bmatrix} + c.c, \tag{34}$$

This manuscript was accepted by Chaos. Click here to see the version of record.

where

$$\gamma = \frac{-a\omega_k^2}{\mu[2i\omega_k - \frac{1-a^2+\epsilon\bar{w}}{\mu} + \frac{1}{2i\omega_k\mu} - \frac{\epsilon}{\mu}e^{-2i\omega_k\tau_k}(w_1\rho_k^2 + \cdots + w_{N-1}\rho_k^{2(N-1)})}. \tag{35}$$

Substituting (30) and (34) into (29), we have that

$$\begin{aligned} &D_0u_3 - N_0u_3 - N_1u_{3\tau} = \\ &-\left[(\mathbf{p_k} - \tau_k N_1\mathbf{p_k}e^{-i\omega_k\tau_k})A_k' - i\omega_k\tau_2 N_1\mathbf{p_k}e^{-i\omega_k\tau_k}A_k - (\frac{i\omega_k^3}{\mu} + \frac{2i\omega_k a\gamma}{\mu}\boldsymbol{\eta})A_k^2\bar{A}_k\right]e^{i\omega_k T_0} + c.c + NRT \end{aligned} \tag{36}$$

Here $\boldsymbol{\eta} = (1, 0, \rho_k, 0, \cdots, \rho_k^{N-1}, 0)^T$, and NRT stands for non-secular terms that do not contribute the normal form. Because the homogeneous part of (36) has nontrivial solutions, the nonhomogeneous equation has a solution only if a solvability condition is satisfied. To determine this solvability condition, we seek a particular solution of (36) in the form

$$u_3(T_0, T_2) = \boldsymbol{\phi}(T_2)e^{i\omega_k T_0} + c.c. \tag{37}$$

and obtain

$$\begin{aligned} &(-i\omega_k I + N_0 + N_1 e^{-i\omega_k\tau_k})\boldsymbol{\phi} = \\ &\quad (\mathbf{p_k} - \tau_k N_1\mathbf{p_k}e^{-i\omega_k\tau_k})A_k' - i\omega_k\tau_2 N_1\mathbf{p_k}e^{-i\omega_k\tau_k}A_k - (\frac{i\omega_k^3}{\mu} + \frac{2i\omega_k a\gamma}{\mu}\boldsymbol{\eta})A_k^2\bar{A}_k). \end{aligned} \tag{38}$$

Note that the problem of finding a solvability condition for the system of different equations (36) has been transformed into finding a solvability condition for the system of algebraic equation (38). Again, because $i\omega_k$ is an eigenvalue of the homogeneous part, (38) has solutions if and only if a solvability condition is satisfied. The condition is that the right-hand side of (38) be orthogonal to every solution of the adjoint homogeneous problem. In this case, the adjoint problem is

$$(N_0^T + N_1^T e^{i\omega_k\tau_k} + i\omega_k I)\mathbf{q_k} = 0. \tag{39}$$

Note that $\mathbf{q_k}$ is not unique. To make it unique, we impose the condition

$$\langle \mathbf{q_k}, \mathbf{p_k} \rangle = \bar{\mathbf{q}_\mathbf{k}}^T\mathbf{p_k} = 1. \tag{40}$$

Thus, we have

$$\mathbf{q_k} = \frac{1}{N(w_k^2 + \frac{1}{\mu})}(i\omega_k, \frac{1}{\mu}, i\omega_k\rho_k, \frac{\rho_k}{\mu}, \cdots, i\omega_k\rho_k^{N-1}, \frac{\rho_k^{N-1}}{\mu}))^T. \tag{41}$$

Taking inner product of the right-hand side of (38) with $\mathbf{q_k}$ yields the solvability condition, which is the normal form

$$A_k' = D_1\tau_2 A_k + D_2 A_k^2 \bar{A}_k, \tag{42}$$

where

$$D_1 = -\frac{i\omega_k^3\epsilon\delta_k e^{-i\omega_k\tau_k}}{\omega_k^2(\mu+\epsilon\delta_k\tau_k e^{-i\omega_k\tau_k})+1}, D_2 \quad = -\frac{\omega_k^4+2\omega_k^2 a\gamma}{\omega_k^2(\mu+\epsilon\delta_k\tau_k e^{-i\omega_k\tau_k})+1}.$$

Let $A_k = r_k e^{i\theta_k}$, substituting these expressions into (42), we have

$$\begin{aligned} r_k' &= d_1\tau_2 r_k + d_2 r_k^3 \\ \theta_k' &= d_3\tau_2 + d_4 r_k^2, \end{aligned} \tag{43}$$

where $d_1 = \mathrm{Re}(D_1), d_2 = \mathbb{R}(D_2), d_3 = \mathrm{Im}(D_1), d_4 = \mathrm{Im}(D_2)$.

This normal form determines both the direction of the Hopf bifurcation (supercritical when $d_1 d_2 < 0$, and subcritical when $d_1 d_2 > 0$), and the stability of bifurcating periodic solutions (stable if $d_2 < 0$, and unstable if $d_2 > 0$).

C. Example: FitzHugh Nagumo network with 6 neurons.

In this section, we illustrate our results by considering specific parameter values: $\mu = 0.1$, $N = 6$ neurons and coupling matrix $W = \mathrm{circ}(0, 1, \frac{1}{2}, \frac{1}{3}, \frac{1}{4}, \frac{1}{5})$.

From Theorems IV.1 and IV.2, for a fixed μ value, the delay independent stability regions can be plotted in the plane of parameters a and ϵ. This is done in Figure (1). In the region marked by GAS, the equilibrium point E^* is globally asymptotically stable for all $\tau \geq 0$. In the region marked by AS, E^* is asymptotically stable. In the region marked by US, E^* is unstable and there is no Hopf bifurcation for any $\tau \geq 0$. In the white region, E^* may be unstable, or experience stability switching when Hopf bifurcation occurs at $\tau = \tau_k$.

From Theorem IV.1, the characteristic equation has at least one root with positive real part for all $\tau \geq 0$ when (a, ϵ) is located on the region marked by US. It follows that periodic orbits created in Hopf bifurcations from E^* in this region are unstable. Thus, Hopf bifurcations creating stable periodic orbits can occur only in the white region. To investigate in further detail, we fix the μ and a values, and plot the Hopf bifurcation curves and stability region in the plane of the coupling strength ϵ and time delay τ. See Figure 2. Then, using Theorem IV.1, we can determine how many pairs of eigenvalues with positive real part there

This manuscript was accepted by Chaos. Click here to see the version of record.

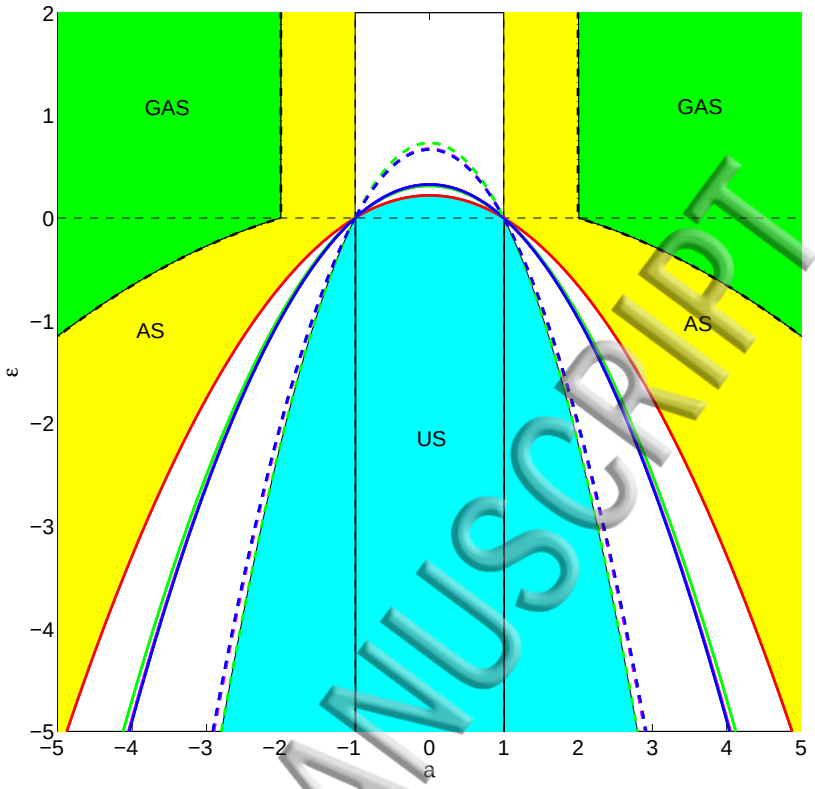

FIG. 1. Delay independent stability of E^* and Hopf bifurcation regions in the $a-\epsilon$ plane for a network of 6 FitzHugh-Nagumo oscillators with $\mu = 0.1$ and connectivity matrix $W = \text{circ}(0, 1, \frac{1}{2}, \frac{1}{3}, \frac{1}{4}, \frac{1}{5})$. In the green shaded region the equilibrium E^* is globally asymptotically stable (GAS), in the yellow shaded region E^* is asymptotically stable (AS), and in the blue shaded region E^* is unstable (US). The red curve is $\epsilon = \frac{1-a^2}{2\bar{w}}$, and the solid (dashed) green, magenta, and blue curves are $\epsilon = \frac{1-a^2}{\bar{w}+|\delta_k|}$ ($\epsilon = \frac{1-a^2}{\bar{w}-|\delta_k|}$) for $k = 1, 2, 3$, respectively.

are in each region of the $\epsilon - \tau$ plane. Hence we can determine the region of stability of E^*; shown by the shaded region in Figure 2. For $a > 1$, region of stability looks similar to that for $a = 1.05$, but as a increases/decreases the Hopf bifurcation curves move to the left/right. When $a = 0.98$ equilibrium point is unstable for all ϵ when $\tau = 0$, but the delay induced Hopf bifurcation stabilizes the equilibrium point in the region shown. As a decreases the curves reorganize and this region of stability is lost for $a < 0.82$.

From the expressions derived in the previous section, we can calculate the sign of the

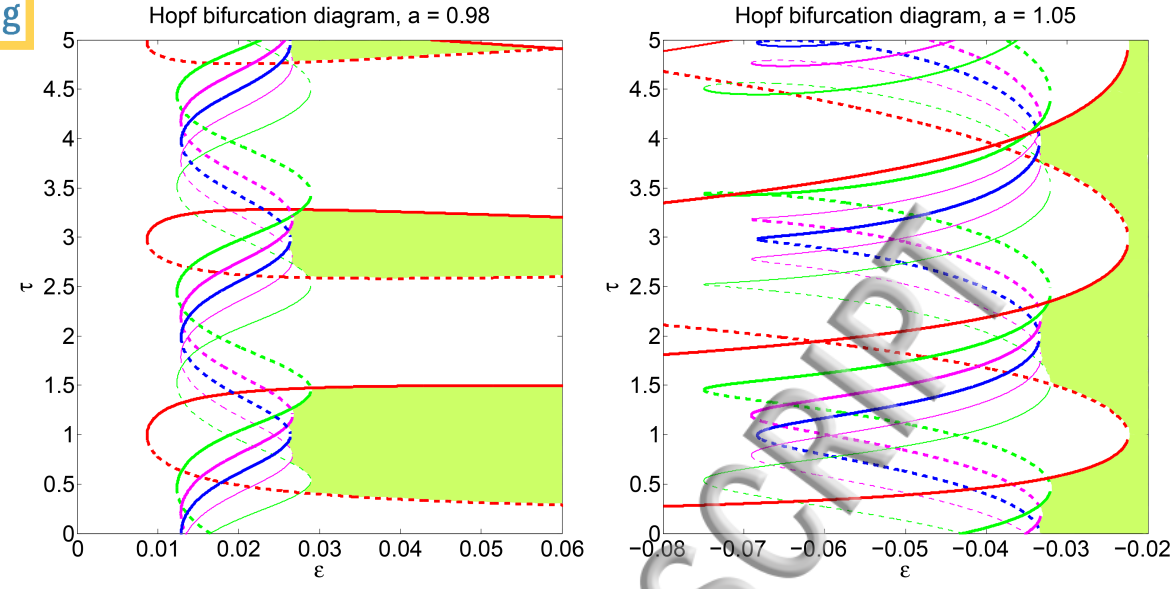

(a) $a = 0.98$ (b) $a = 1.05$

FIG. 2. Hopf bifurcation curves for the system (17) with $N = 6$ neurons. Red, green, magenta, blue curves are Hopf bifurcation curves for $k = 0, 1, \cdots, 3$, (corresponding to 1-cluster, 6-cluster, 3-cluster and 2-cluster periodic solutions), respectively. Thin (thick) dashed curves correspond to $\tau^-_{k,j}(\hat{\tau}^-_{k,j})$. Thin (thick) solid curves correspond to $\tau^+_{k,j}(\hat{\tau}^+_{k,j})$. In the green shaded region the equilibrium E^* is asymptotically stable. Parameter values are $\mu = 0.1$, $W = \text{circ}(0, 1, \frac{1}{2}, \frac{1}{3}, \frac{1}{4}, \frac{1}{5})$ and a values as shown.

coefficients d_1, d_2 of the normal form (42), at each critical τ value along the Hopf bifurcation curves of Figure 2. Note that the sign of d_1 is the same as that of $d\text{Re}(\lambda)/d\tau$ thus it is positive at the $\tau^+_{k,j}$ bifurcations (solid curves in Figure 2) and negative at the $\tau^-_{k,j}$ bifurcations (dashed curves in Figure 2). The sign of d_2 varies. For $a = 0.98$, all the $\tau^-_{k,j}$ bifurcations have $d_2 < 0$. However, d_2 changes sign along the $\tau^+_{k,j}$ bifurcation curves. For the 1-cluster Hopf (red, dashed curve) $d_2 > 0$ for most of the curve, while for the other Hopfs generally $d_2 < 0$ on the portions of the curves which form the boundary of the stability region. This indicates that the 2, 3 and 6-cluster Hopf bifurcations that lie next to the region of stability give rise to stable periodic orbits while the 1-cluster Hopf bifurcations gives rise to stable periodic orbits along the solid curves and unstable periodic orbits along the dashed curves.

In the following, we illustrate how the coupling time delay affects the stability of the equilibrium point E^* and the cluster periodic solutions arising in the Hopf bifurcations by

This manuscript was accepted by Chaos. Click here to see the version of record.

considering $a = 0.98$ and four values of ϵ. We compare predictions of the theory with numerical continuation with respect to τ carried out with DDE-BIFTOOL[45], and numerical simulations for some specific τ values with initial conditions

$$x_i(t) = x^* + 0.5RD - 0.5RD,$$
$$y_i(t) = y^* + 0.5RD - 0.5RD, \ t \in [-\tau, 0],$$

where RD is any random number between $[0, 1]$.

For $\epsilon = 0.04$, the sequence of τ bifurcation values (rounded to two decimal places) is

$$0 < \tau^-_{0,1}(0.35) < \tau^+_{0,1}(1.49) < \tau^-_{0,2}(2.58) < \tau^+_{0,2}(3.26) < \tau^-_{0,3}(4.82) < \tau^+_{0,3}(5.02).$$

The theory predicts that the equilibrium point E^* is stable for $\tau \in (0.35, 1.49) \cup (2.58, 3.26) \cup (4.82, 5.02)$ and unstable elsewhere. Further, stable 1-cluster periodic orbits are predicted for τ greater than but sufficiently close to $\tau^+_{0,1}, \tau^+_{0,2}, \tau^+_{0,3}$ and unstable 1-cluster periodic orbits for τ greater than but sufficiently close to $\tau^-_{0,1}, \tau^-_{0,2}, \tau^-_{0,3}$. These predictions are confirmed by the numerical simulations. The simulations also show that a large amplitude stable 1-cluster solution exists for $\tau \in (0, 0.46) \cup (4.15, 5)$. Numerical continuation further confirms the theoretical predictions and shows how the large amplitude 1-cluster solutions are connected to the 1-cluster solutions created by the Hopf bifurcation (see Figure 3(a)). For example, there is a saddle node of limit cycles near $\tau = 0.5$ connecting the 1-cluster solution which exists for τ near 0 with the Hopf bifurcation at $\tau^-_{0,1}$. Numerical simulations also show that nonsymmetric cluster solutions exist for $\tau \in (\tau^+_{0,1}, \tau^-_{0,2}) \cup (\tau^+_{0,2}, \tau^-_{0,3})$ (see Figure 7 (b) for an example).

For $\epsilon = 0.0285$, we focus on $\tau < 3$. Note that, in this case, no stable 6-cluster solutions bifurcate from any $\tau^{\pm}_{1,j}(\tilde{\tau^{\pm}_{1,j}}) > 3$. The theory predicts a stable equilibrium for $\tau \in (\tau^-_{0,1}(0.41), \tau^+_{1,0}(0.46)) \cup (\tau^-_{1,0}(0.61), \hat{\tau}^+_{1,1}(1.37)) \cup (\tau^-_{1,1}(2.61), \tau^+_{0,2}(3.28))$, a stable 6-cluster periodic orbit for $\tau \gtrapprox \tau^+_{1,0}(0.46)$, $\tau \lessapprox \tau^-_{1,0}(0.61)$, $\tau \gtrapprox \hat{\tau}^+_{1,1}(1.37)$, $\tau \lessapprox \tau^-_{1,1}(2.61)$. This is confirmed by the numerical simulations. See Figure 4 for some examples. Note that the large amplitude 1-cluster solutions are observed here as well. Numerical continuation further confirms the theoretical predictions (see Figure 3(b)). It also shows that the large amplitude 1-cluster solutions are created in a similar way to $\epsilon = 0.04$, although the 1-cluster Hopf bifurcations all give rise to unstable periodic orbits.

Similar analysis predicts τ values where stable 6-cluster and 3-cluster periodic solutions exist for $\epsilon = 0.0266$, and stable 3-cluster and 2-cluster periodic solutions for $\epsilon = 0.0263$. In

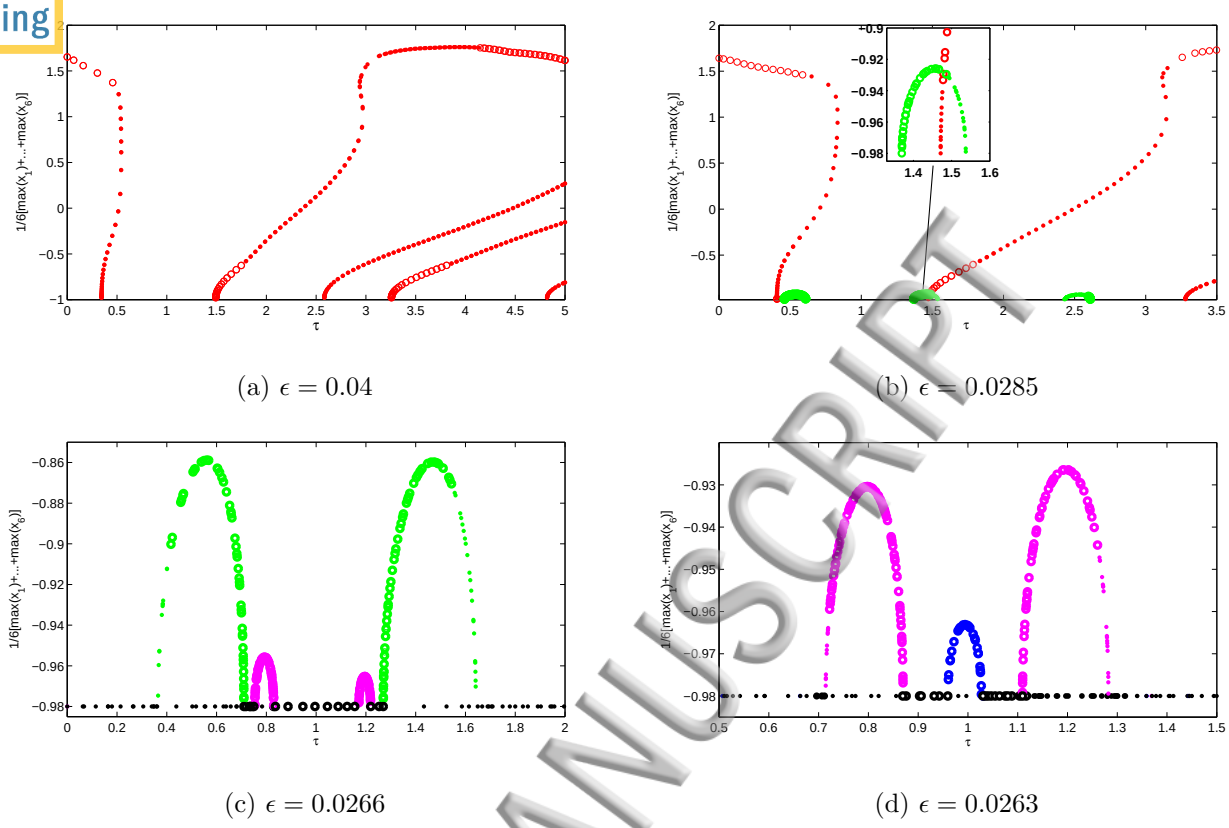

(a) $\epsilon = 0.04$ (b) $\epsilon = 0.0285$

(c) $\epsilon = 0.0266$ (d) $\epsilon = 0.0263$

FIG. 3. Branches of symmetric cluster periodic solutions from numerical continuation with respect to τ with ϵ values as shown. Other parameter values are as in Figure 2(a). Circles (dots) correspond to stable (unstable) solutions. Red/green/magenta/blue correspond to 1-cluster/6-cluster/3-cluster/2-cluster periodic solutions. Black corresponds to the equilibrium point, E^*.

both cases, the numerical simulations and numerical continuation agree with the analysis. See Figure 3(c),(d) for numerical continuations and Figure 5 for numerical simulations for $\epsilon = 0.0263$.

V. CONCLUSION

In this paper, we investigated Hopf bifurcations of a general network of N globally coupled identical nodes with time delayed coupling. We derived expressions for all delay induced Hopf bifurcations from a symmetric equilibrium point and used symmetric bifurcation theory to determine the cluster periodic solutions which are created by these bifurcations. Our results

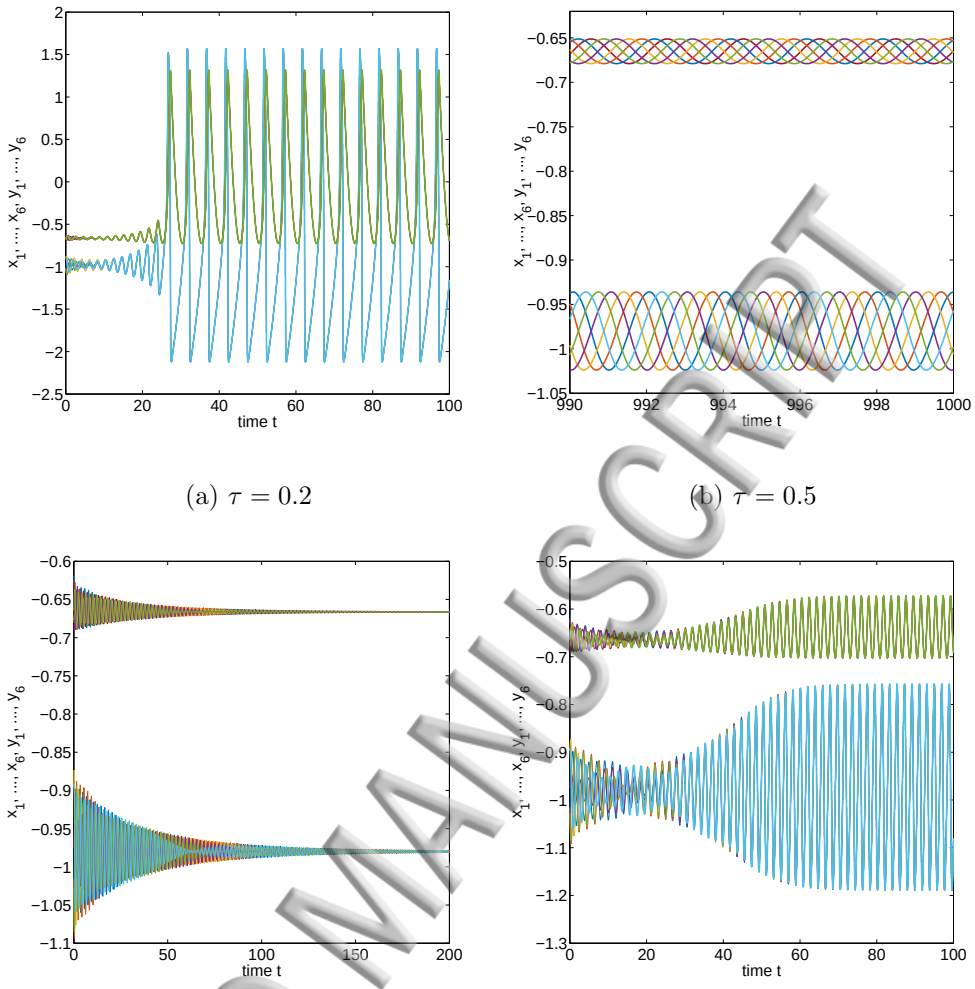

(a) $\tau = 0.2$ (b) $\tau = 0.5$

(c) $\tau = 1.0$ (d) $\tau = 1.6$

FIG. 4. Numerical simulations showing stable behaviour for $\epsilon = 0.0285$ and τ values as shown. Other parameter values are as in Figure 2(a). In each plot the upper traces correspond to $y_1, \ldots, y_6$ and the lower traces to $x_1, \ldots, x_6$. (a) In-phase (1-cluster) periodic orbit. (b) 6-cluster periodic orbit. (c) Equilibrium point, E^*. (d) In-phase periodic orbit.

apply to most typical neural network models, including both biophysical (conductance-based) and artificial networks.

We applied our results to a particular model: a network of FitzHugh-Nagumo neurons with delayed, diffusive coupling. We completely described the delay independent stability of the symmetric equilibrium point and the delay induced Hopf bifurcations. We gave explicit expressions for the critical delay values, showing how these depend on other parameters, including the coupling strength and the parameter (a) that induces oscillations in the un-

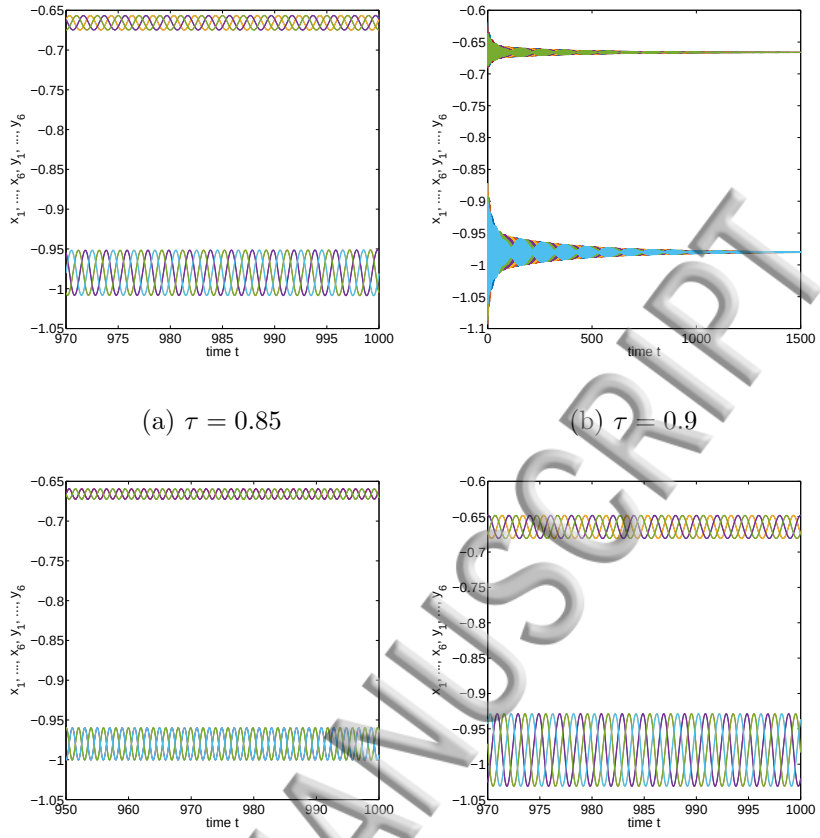

(a) $\tau = 0.85$ (b) $\tau = 0.9$

(c) $\tau = 1.0$ (d) $\tau = 1.2$

FIG. 5. Numerical simulations showing stable behaviour for $\epsilon = 0.0263$ and τ values as shown. Other parameter values are as in Figure 2(a). In each plot the upper traces correspond to $y_1, \ldots, y_6$ and the lower traces to $x_1, \ldots, x_6$. (a) 3-cluster periodic orbit. (b) Equilibrium point, E^*. (c) 2-cluster periodic orbit. (d) 3-cluster periodic orbit.

coupled neural model. Further, using the method of multiple scales, we explicitly derived the normal forms at Hopf bifurcation critical points, which determine the direction of Hopf bifurcation and stability of bifurcating periodic orbits.

We illustrated our results for specific parameter values in the example model, focussing on the case of 6 neurons. We presented curves of Hopf bifurcations in the parameter space consisting of the coupling delay and coupling strength and studied how these curves change as the parameter a is varied. We showed that Hopf bifurcations leading to stable cluster solutions could occur both in the case where the neurons are intrinsically oscillating and when they are not. Theoretical results, confirmed by numerical continuation and numerical simulations, indicate that increasing the time delay can cause the stable solution to switch

This manuscript was accepted by Chaos. Click here to see the version of record.

between the equilibrium solution and $1, 2, 3$ or $6-$ cluster periodic orbits.

We note that symmetric bifurcations exist in the coupled system with no delay, but occur in a strict ordering in parameter space. The delay causes variation in the ordering of the curves, allowing for bifurcation of stable solutions of all cluster types. Further, this reordering gives rise to intersection points of the various Hopf bifurcations, which correspond to co-dimension two Hopf-Hopf bifurcation points. Such points, which are quite common in delay systems[35,46], can lead to coexistence of multiple stable periodic solutions or tori[47]. Indeed, in other numerical simulations we have found bistability between symmetric cluster solutions (Figure 6) and stable torus solutions (Figure 7(a)).

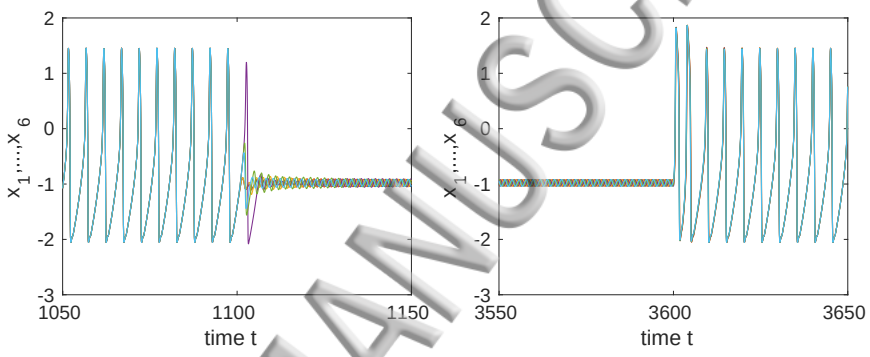

(a) $\Delta a = 0.05,\ 1100 \leq t \leq 1105,$ neurons $1, 2, 3.$

(b) $\Delta a = -0.2,\ 3600 \leq t \leq 3605,$ all neurons

FIG. 6. Numerical simulations showing bistability between a large amplitude 1-cluster solution and a small amplitude 6-cluster solution. Parameter values are as in Figure 2(a) with $\epsilon = 0.027,\ \tau = 0.65$. Initial conditions were constant on $t \in [-\tau, 0]$ with values as follows (a) $x_j = 1,\ j = 1, \ldots, 6,\ y_1 = -0.45, y_j = -0.4,\ j = 2, \ldots, 6$; (b) $x_1 = -0.9, x_j = -0.9,\ j = 2, \ldots, 6,\ y_1 = -0.45, y_j = -0.4,\ j = 2, \ldots, 6$. Switching between the attractors is achieved by applying a short term perturbation to the parameter a as indicated in the captions.

As previously noted, other solutions not predicted by our results occur (see Figure 7(b)). The origin of such solutions is a topic for future work.

The delay-induced Hopf bifurcations in the case study we considered are linked to super-critical Hopf bifurcations in the uncoupled neurons. This can be seen as follows. Taking $\tau^{\pm}_{k,0}$ to zero, implies that $\epsilon(\alpha_k - \bar{w}) + 1 - a^2 = 0$, which is the Hopf bifurcation condition for the nondelayed system (see Lemma IV.1 and Figure 2). Further, as ϵ goes to zero we obtain the Hopf bifurcation condition in the uncoupled neuron, $1 - a^2 = 0$. Thus the cluster

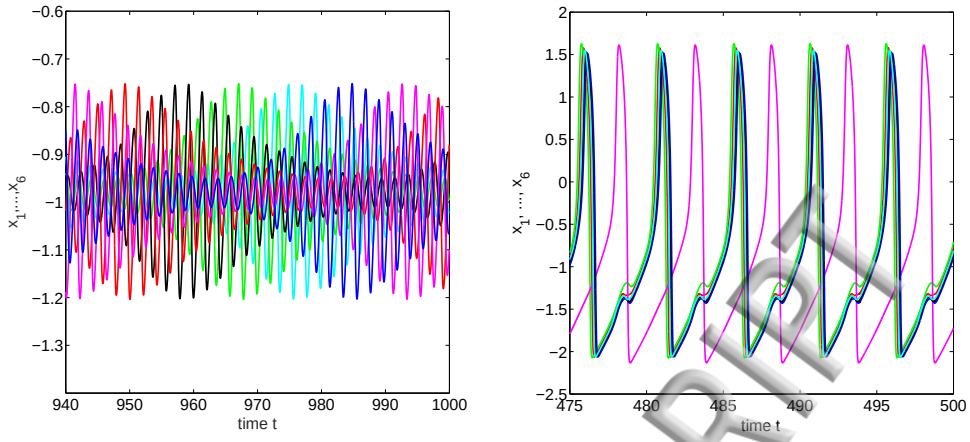

(a) $\epsilon = 0.021, \tau = 1.4$ (b) $\epsilon = 0.04, \tau = 2.2$

FIG. 7. Numerical simulations showing stable solutions not predicted by theory. Parameter values are as in Figure 2(a) with ϵ and τ as shown. (a) 6-cluster torus. (b) Non-symmetric cluster periodic orbit.

patterns can be thought of as emanating from an interaction of the delay with the intrinsic oscillation mechanism of the neurons. In neural models exhibiting Type II excitability, where oscillations are created by a subcritical Hopf bifurcations, we expect that a similar mechanism for creating cluster patterns can occur. In neural models exhibiting Type I excitability, however, oscillations are created by a saddle node on an invariant circle (SNIC) bifurcations. Nevertheless, delay induced cluster patterns are still observed[13]. Since most Type I model neurons have a Hopf bifurcation involved in the destruction of limit cycles we conjecture that the mechanism we have discussed may still come into play.

REFERENCES

[1]D. Hansel, G. Mato, and C. Meunier, Europhys. Lett. **23**, 367 (1993).
[2]N. Kopell and G. Ermentrout, Math. Biosci. **90**, 87 (1988).
[3]H. Winful and S. Wang, Appl. Phys. Lett. **52**, 1774 (1988).
[4]H. Winful and S. Wang, Applied Physics Letters **53**, 1894 (1988).
[5]R. Mirollo and S. Strogatz, SIAM J. Appl. Math. **50**, 1645 (1990).
[6]A. Takamatsu, T. Fujii, and I. Endo, Phys. Rev. E **85**, 2026 (2000).
[7]F. Dörfler and F. Bullo, Automatica **50**, 1539 (2014).

[8]D. Paré, R. Curro'Dossi, and M. Steriade, Neuroscience **35**, 217 (1990).

[9]K. Okuda, Physica D **63**, 424 (1993).

[10]D. Golomb and J. Rinzel, Physica D **72**, 259 (1994).

[11]P. Bressloff and S. Coombes, Physica D **126**, 99 (1999).

[12]P. Bressloff and S. Coombes, Physica D **130**, 232 (1999).

[13]Z. Wang and S. A. Campbell, in *12th IFAC Workshop on Time Delay Systems* (2015) pp. 105–110.

[14]S. A. Campbell and Z. Wang, arXiv preprint arXiv:1607.05759 (2016).

[15]S. Crook, G. Ermentrout, M. Vanier, and J. Bower, J. Comp. Neurosci. **4**, 161 (1997).

[16]J. Cao and L. Li, Neural Networks **22**, 335 (2009).

[17]C.-U. Choe, T. Dahms, P. Hövel, and E. Schöll, Phys. Rev. E **81**, 025205 (2010).

[18]T. Dahms, J. Lehnert, and E. Schöll, Phys. Rev. E **86**, 016202 (2012).

[19]G. Orosz, in *10th IFAC Workshop on Time Delay Systems* (2012) pp. 173–178.

[20]G. Orosz, in *Delay Systems* (Springer, 2014) pp. 343–357.

[21]G. Orosz, SIAM J. Applied Dynamical Systems **13**, 1353 (2014).

[22]N. Burić and D. Todorović, Phys. Rev. E **67**, 066222 (2003).

[23]N. Burić, I. Grozdanović, and N. Vasović, Chaos, Solitons and Fractals **23**, 1221 (2005).

[24]S. A. Campbell, R. Edwards, and P. van den Dreissche, SIAM J. Applied Mathematics **65**, 316 (2004).

[25]Y. Song and J. Xu, IEEE Transactions on Neural Networks and Learning Systems **23**, 1659 (2012).

[26]M. Golubitsky, I. Stewart, and D. G. Scherffer, *Singularities and Groups in Bifurcation Theory* (Springer-Verlag, New York, 1988).

[27]J. Wu, Trans. Amer. Math. Soc. **350**, 4799 (1998).

[28]S. A. Campbell, I. Ncube, and J. Wu, Physica D **214**, 101 (2006).

[29]S. Guo, L. Huang, and L. Wang, Internat. J. Bifur. Chaos **14**, 27992810 (2004).

[30]S. Guo and L. Huang, Physica D **183**, 19 (2003).

[31]I. Ncube, S. A. Campbell, and J. Wu, Fields Inst. Commun. **36**, 17 (2003).

[32]S. D. Bungay and S. A. Campbell, International J. Bifurcation and Chaos **17**, 3109 (2007).

[33]S. Guo and L. Huang, J. Differential Equations **236**, 343 (2007).

[34]J. Ying and Y. Yuan, Nonlinear Analysis: Real World Applications **14**, 1102 (2013).

[35]J. Ying and Y. Yuan, J. Mathematical Analysis and Applications **425**, 1155 (2015).

[36]P.-L. Buono and J. A. Collera, SIAM J. Applied Dynamical Systems **14**, 1868 (2015).

[37]K. B. Blyuss and Y. N. Kyrychko, Bulletin of Mathematical Biology **74**, 2488 (2012).

[38]K. B. Blyuss, J. Mathematical Biology **66**, 115 (2013).

[39]K. B. Blyuss, J. Mathematical Biology **69**, 1431 (2014).

[40]G. J. Tee, Res. Lett. Inf. Math. Sci. **8**, 123 (2005).

[41]S. A. Campbell, Y. Yuan, and S. D. Bungay, Nonlinearity **18**, 2827 (2005).

[42]J. Hale and S. Verduyn Lunel, *Introduction to Functional Differential Equations* (Springer Verlag, New York, 1993).

[43]R. FitzHugh, Biophysical J. **1**, 445 (1961).

[44]J. Nagumo, S. Arimoto, and S. Yoshizawa, Proceeding IRE **50**, 20612070 (1962).

[45]K. Engelborghs, T. Luzyanina, and G. Samaey, "DDE-BIFTOOL v. 2.00: a MATLAB package for bifurcation analysis of delay differential equations." Tech. Rep. TW-330 (Department of Computer Science, K.U. Leuven, Leuven, Belgium, 2001).

[46]J. Bélair and S. A. Campbell, SIAM J. Appl. Math. **54**, 1402 (1994).

[47]J. Guckenheimer and P. Holmes, *Nonlinear Oscillations, Dynamical Systems and Bifurcations of Vector Fields* (Springer-Verlag, New York, 1983).

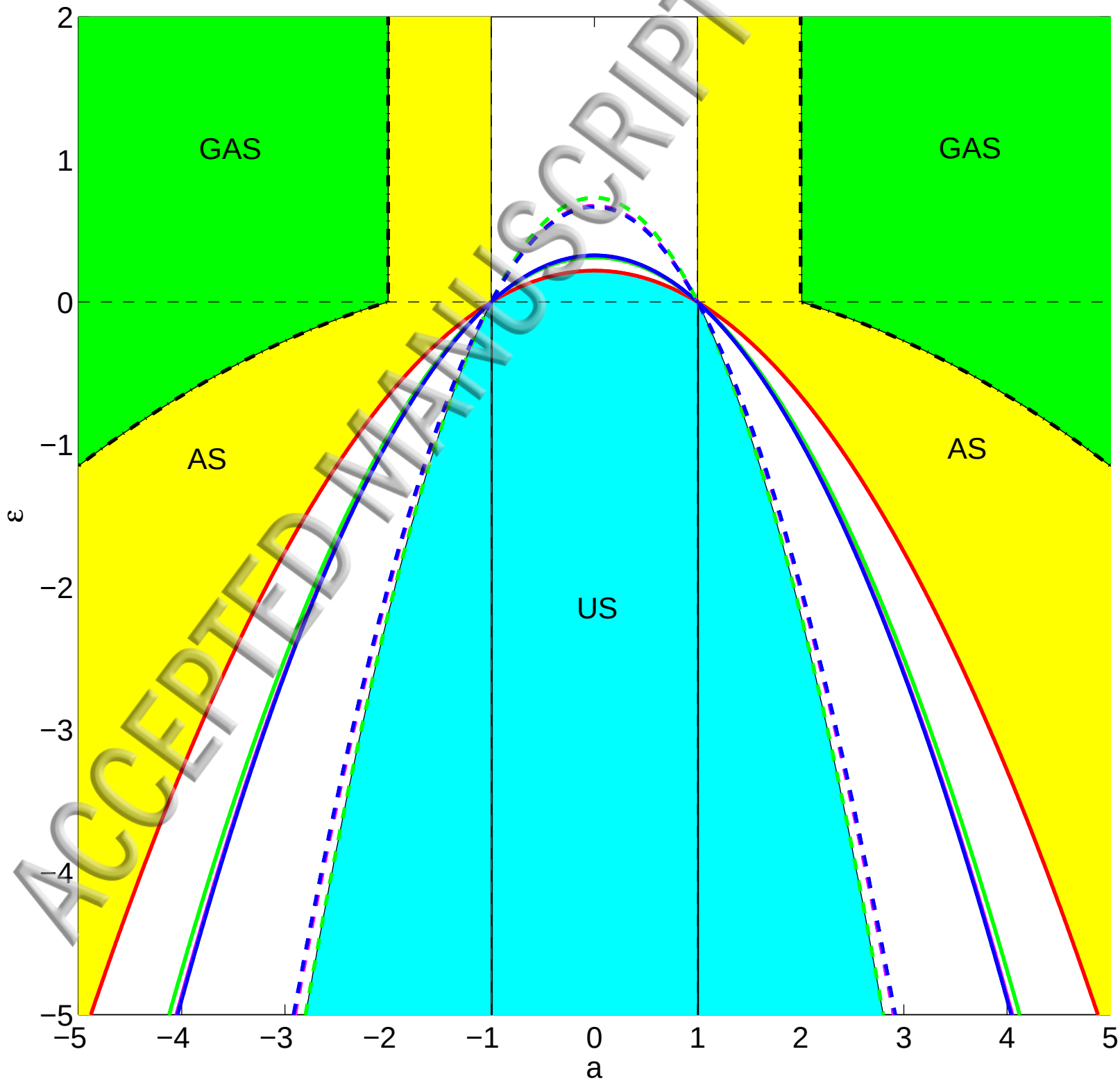

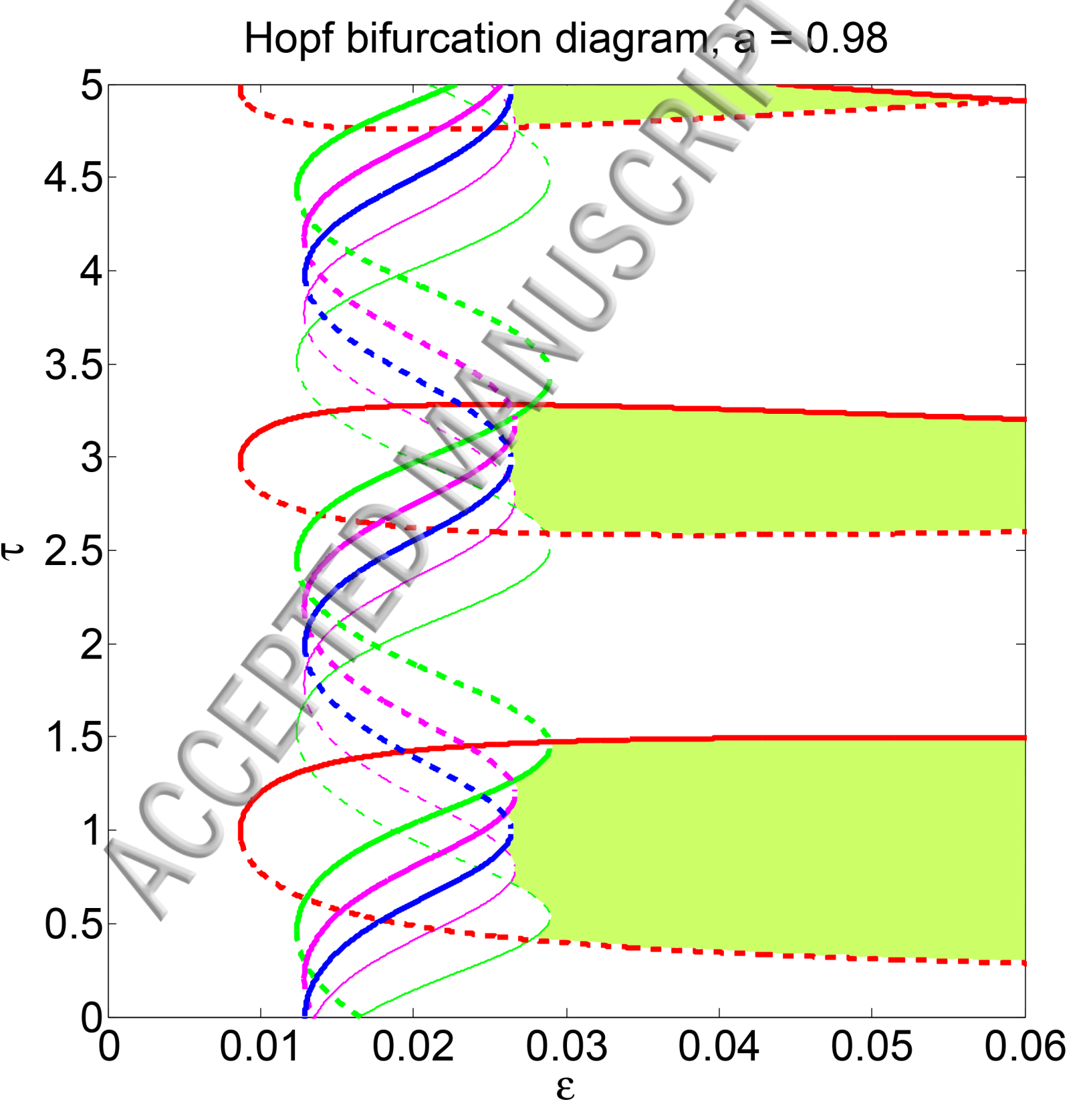

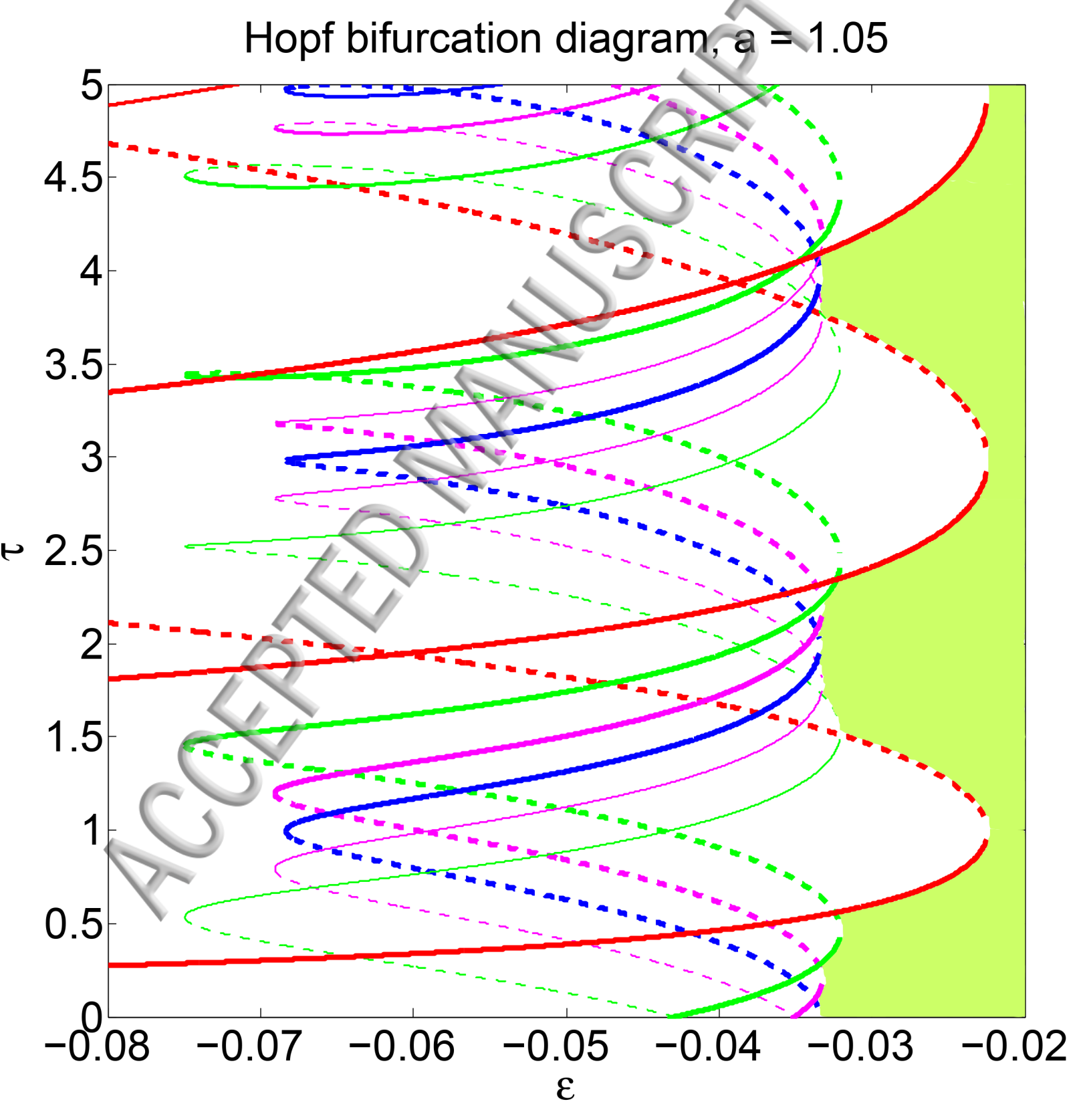

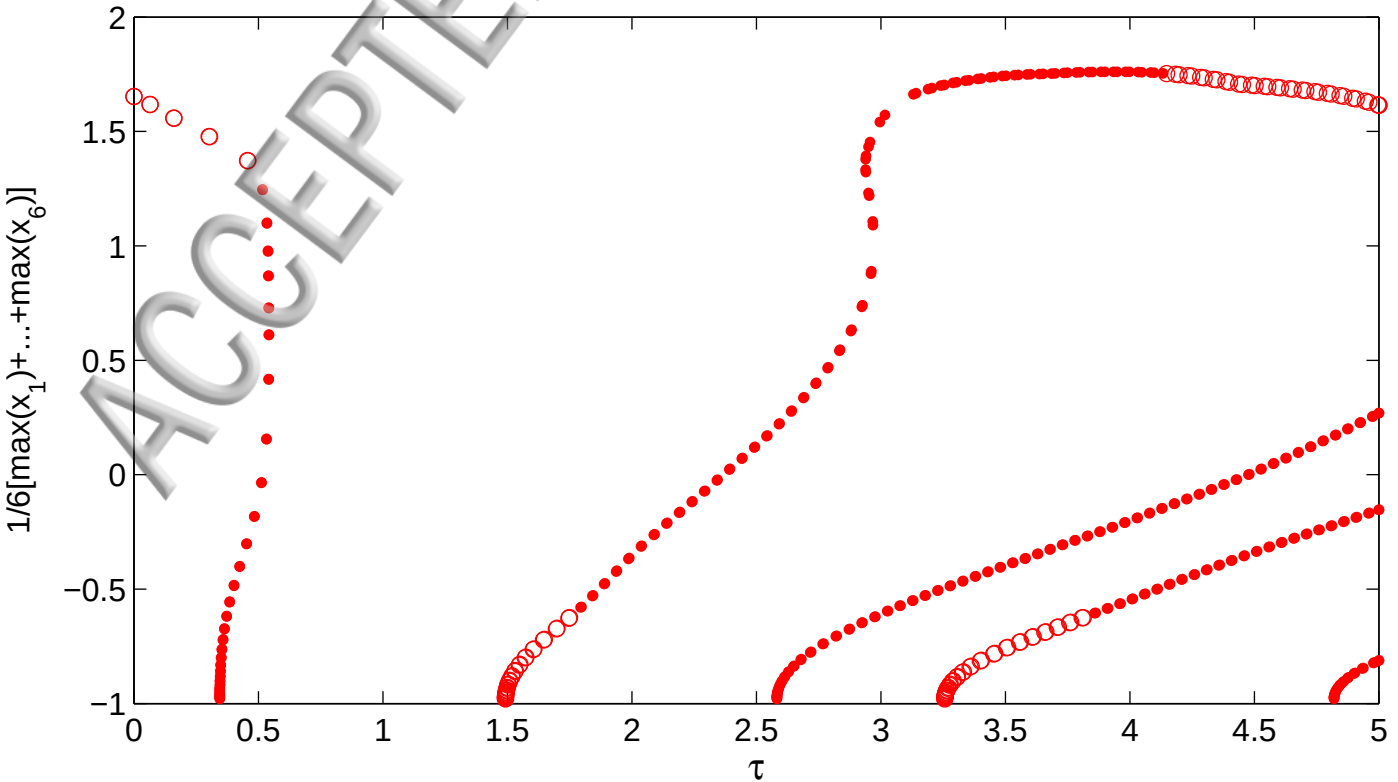

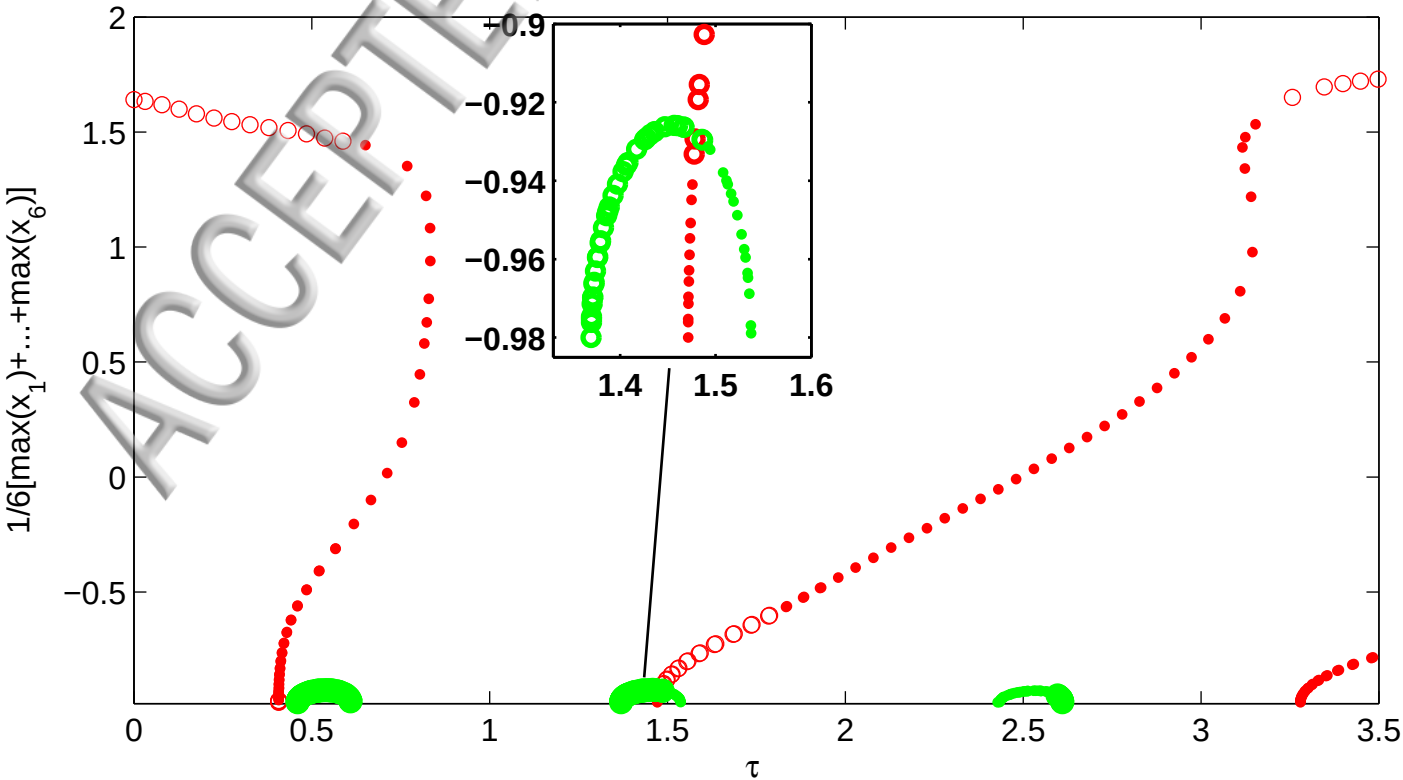
1/6[max(x1)+...+max(x6)]
τ
2
1.5
1
0.5
0
−0.5
0
0.5
1
1.5
2
2.5
3
3.5
−0.9
−0.92
−0.94
−0.96
−0.98
1.4
1.5
1.6

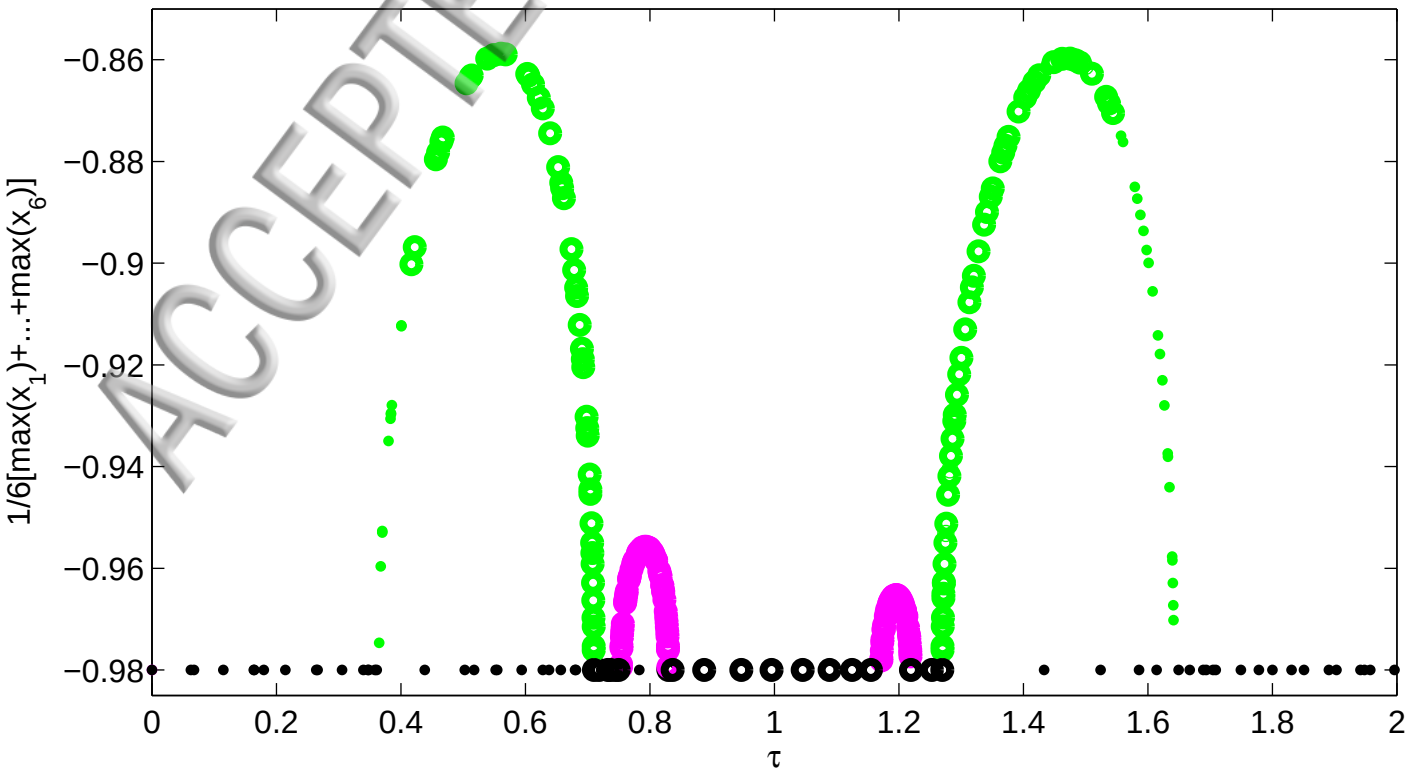
−0.86
−0.88
−0.9
−0.92
−0.94
−0.96
−0.98
1/6[max(x1)+...+max(x6)]
0
0.2
0.4
0.6
0.8
1
1.2
1.4
1.6
1.8
2
τ

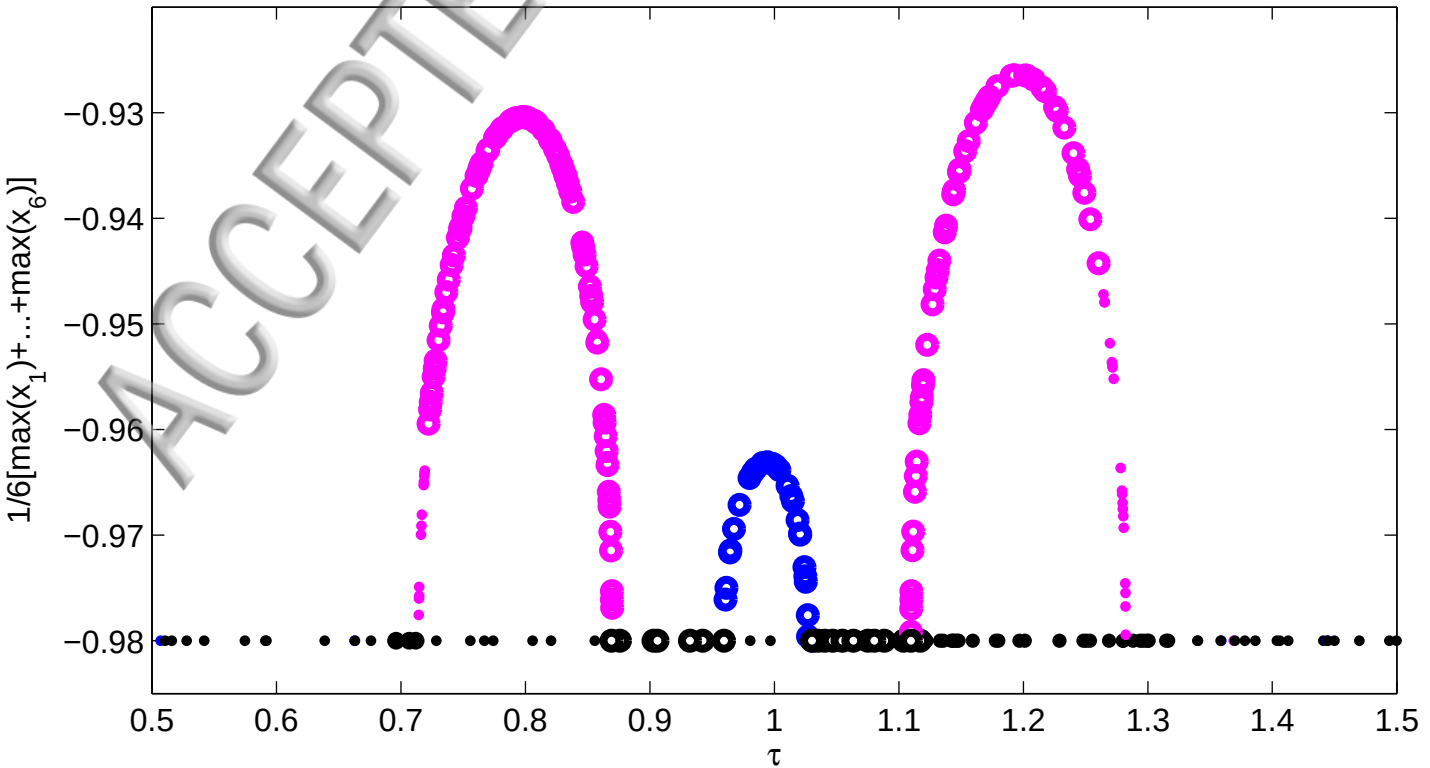
−0.93
−0.94
−0.95
−0.96
−0.97
−0.98
1/6[max(x1)+...+max(x6)]
0.5
0.6
0.7
0.8
0.9
1
1.1
1.2
1.3
1.4
1.5
τ